

A statistical theory of structure in many-particle systems with local interactions

John Çamkiran,^{1,*} Fabian Parsch,^{2,1} and Glenn D. Hibbard¹

¹*Department of Materials Science and Engineering, University of Toronto, Toronto, Ontario, M5S 3E4, Canada*

²*Department of Mathematics, University of Toronto, Toronto, Ontario, M5S 2E4, Canada*

(Dated: February 12, 2026)

A theory of structure is formulated for systems of many structureless classical particles with stable local interactions in Euclidean space. Such systems are shown to have their structure in thermodynamic equilibrium determined exactly by a random field of fine local descriptions and approximately by coarsenings thereof. The degree of order in the local cluster consisting of a particle and its neighbors is identified as a universal source of coarse local descriptions and characterized by expressing the behavior of configurational entropy in local microscopic terms. A local measure of the angular redundancy in neighboring particle positions is found to satisfy this characterization and thereby established as a valid local order quantifier. A precise relationship between order and symmetry is obtained by bounding this quantifier sharply from below by a simple function of the local point group and the largest stabilizer under its action on the set of bond pairs. The marginal distribution of the quantifier is given in closed form for highly coordinated particles with broadly distributed bond angles. Applications are made to the ideal gas, perfect crystal, and simple liquid.

I. INTRODUCTION

More than a century after the advent of x-ray diffraction, our understanding of structure in condensed matter remains largely phase-specific. With at least one fundamental limitation on what properties can be evaluated by direct simulation [1–3], a broader theory of structure will be essential to furthering our ability to explain and predict the behavior of many-particle systems.

The early results of crystallography provide a special theory of structure grounded in the geometry of lattices and the algebra of discrete groups [4–6]. Reciprocal-space methods extend the scope of our understanding to noncrystalline systems [7–9] yet do so at the expense of spatial resolution [10–12]. To address this shortcoming, such methods have been complemented with real-space descriptors to great practical effect [12–15] but without substantial progress toward a general invariant of structure that is at once complete and tractable.

Indeed traditional invariants of structure are beset by the problem that they are either complete or tractable but not in general both. Perfect crystals at absolute zero are one setting in which the former can be attained without forgoing the latter. Outside that setting, the pair correlation function affords some degree of tractability [16, 17]. Yet in neglecting the higher-order dependencies that are often of importance [18–22], such two-particle descriptions lack completeness except in special cases [23–25]. And while the n -particle distribution function is trivially complete for sufficiently large n , its estimation suffers acutely from the curse of dimensionality [26].

The use of novel local descriptors has emerged as a promising alternative in the face of the dilemma inherent in traditional approaches [12, 15]. Despite its empirical successes, however, this practice has yet to be placed on a firm theoretical foundation.

The present work arrives at a collection of results that formally concern systems of many structureless classical particles with stable local interactions but that nevertheless provide a perspective on all assemblies of countably many bodies described entirely by their species, positions, and momenta. Proceeding from classical theory, it is shown that the equilibrium structure of such systems can in principle be determined from little more than sufficiently rich local descriptions. Building on more recent findings, a definition for a local order quantifier is developed with reference to the behavior of configurational entropy as expressed in local microscopic terms. From there we derive a local measure of the angular redundancy in neighboring particle positions, which in satisfying that definition affords a natural means of describing structure at the length scale of interparticle interactions.

The remainder of the paper is organized as follows: Sec. II grounds the work in a treatment of structure and order in thermodynamic equilibrium; Sec. III introduces a practical local order quantifier in the more general setting, establishes with its help a precise relationship between order and symmetry, and obtains an expression for its marginal distribution in closed form; Sec. IV closes with a few elementary applications.

II. STRUCTURE AND ORDER

The extent to which the structure of a classical many-particle system can be captured with local descriptions is a question that remains unresolved notwithstanding the progress made [27–31]. We address this problem in the following discussion by providing a sufficient condition under which local descriptions give rise to a complete structural invariant and consider the approximability of such an invariant when that condition is not strictly satisfied. Later we identify the local degree of order as a source of local descriptions that is universally available.

* john.camkiran@utoronto.ca

A. Describing structure

It is a familiar quality of systems with a large number of particles that nontrivial global structures can arise from strictly local interactions. In order to be able to discuss the description of structure in that setting, we must first make the notion of a local interaction precise. Throughout the work we call an interaction *local* if it involves, in addition to a particle, one or more of its neighbors as given by some deterministic rule.

1. Configurational probability density

Consider a system of N structureless classical particles in Euclidean space \mathbb{R}^D with interactions that are stable and local with respect to a symmetric irreflexive configuration-dependent and isometry-invariant neighbor relation \sim . Suppose that no external fields are present.

By its locality, every interaction is supported on a set of particles that induces a radius-1 subgraph of the \sim -neighbor graph $G(\mathcal{X})$, given for each configuration \mathcal{X} by

$$G(\mathcal{X}) = (I, \{\{i, j\} \in \binom{I}{2} : i \sim j\}),$$

where $I = \{1, \dots, N\}$ and $\binom{I}{2}$ is the set of all (unordered) pairs in I . A few radius-1 graphs are illustrated in Fig. 1.

Denote by $\mathcal{R}(G(\mathcal{X}))$ the set comprising the vertex sets of all induced radius-1 subgraphs of $G(\mathcal{X})$ that support an interaction. The potential energy is then given by

$$U(\mathcal{X}) = \sum_{R \in \mathcal{R}(G(\mathcal{X}))} \Psi(\mathcal{X}_R), \quad (1)$$

where \mathcal{X}_R is the restriction of the configuration \mathcal{X} to the set R and Ψ is an isometry-invariant interaction potential. By stability $U(\mathcal{X}) \geq CN$ for some $C \in (-\infty, 0]$ for all \mathcal{X} [32]. We require also that $\Psi(\mathcal{X}_R) \geq c_R$ for some $c_R \in (-\infty, 0]$ for every R . Thus standard pair, multi-body, and embedded-atom potentials are all possible Ψ .

If the system is in canonical equilibrium at temperature T while confined to a region of volume V , then its configurational probability density function f_X is given for all admissible configurations $\mathcal{X} \in \Gamma \subseteq (\mathbb{R}^D)^N$ by

$$\begin{aligned} f_X(\mathcal{X}) &= \frac{1}{Z} \exp(-\beta U(\mathcal{X})) \\ &\propto \exp \left\{ -\beta \sum_{R \in \mathcal{R}(G(\mathcal{X}))} \Psi(\mathcal{X}_R) \right\} \\ &= \prod_{R \in \mathcal{R}(G(\mathcal{X}))} \exp(-\beta \Psi(\mathcal{X}_R)) \\ &= \prod_{R \in \mathcal{R}(G(\mathcal{X}))} \psi(\mathcal{X}_R), \end{aligned} \quad (2)$$

where $Z = \int_{\Gamma} \exp(-\beta U(\mathcal{X})) d\mathcal{X}$ is the canonical configurational partition function, $\beta = 1/(k_B T)$ is the inverse temperature, k_B is the Boltzmann constant, and $\psi(\mathcal{X}_R) := \exp(-\beta \Psi(\mathcal{X}_R))$ is the Boltzmann factor.

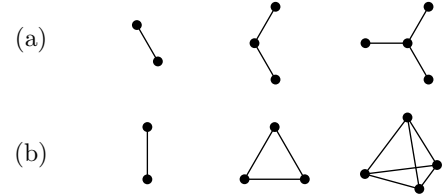


FIG. 1. Radius-1 graphs include (a) star graphs and (b) complete graphs, but also wheel graphs, fan graphs, and others.

2. Fine local descriptions

Structural descriptions are only truly local if they cannot be used to reconstruct the global configuration given the neighbor graph and are fine if they recover the Boltzmann factors. We formalize these notions below.

Let $w = (w_i)_{i \in I}$ be an indexed family of particle-centered descriptions for a configuration \mathcal{X} . The descriptions w_i are *local* if they are the images $g(\mathcal{X}_i)$ of the restricted configurations

$$\mathcal{X}_i := (x_j)_{j=i \text{ or } j \sim i}$$

under a common function g for all $\mathcal{X} \in \Gamma$ such that $(w, G(\mathcal{X}))$ does not in general determine \mathcal{X} for connected $G(\mathcal{X})$ up to Euclidean motions. The descriptions w_i are *fine* if there exists a common function τ for all $\mathcal{X} \in \Gamma$ satisfying, for every $R \in \mathcal{R}(G(\mathcal{X}))$, the equality

$$\tau(w_R) = \psi(\mathcal{X}_R), \quad w_R := (w_i)_{i \in R}. \quad (3)$$

An example of fine local descriptions is given by the sets of all labeled pairwise distances near each particle i ,

$$\mathcal{D}_i = \{(\{j, k\}, \|x_j - x_k\|) : j \sim i, (k = i \text{ or } k \sim i), k \neq j\}.$$

Indeed by classical distance geometry such descriptions recover, up to Euclidean motions, the restricted configuration \mathcal{X}_i and therefore the Boltzmann factors $\psi(\mathcal{X}_R)$ but do not in general determine the global configuration \mathcal{X} . By contrast the sets of all labeled neighbor vectors,

$$\mathcal{V}_i = \{(j, x_j - x_i) : j \sim i\},$$

are fine but not local, since $((\mathcal{V}_i)_{i \in I}, G(\mathcal{X}))$ determines \mathcal{X} up to a translation if $G(\mathcal{X})$ is connected. Fig. 2 illustrates these two classes of descriptions along with a third.

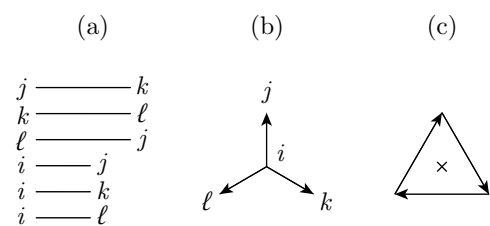


FIG. 2. Three classes of structural descriptions: (a) labeled pairwise distances (fine local); (b) labeled neighbor vectors (fine nonlocal); (c) inter-neighbor vectors (non-fine local).

Together Eqs. (2) and (3) imply that

$$\begin{aligned} f_X(\mathcal{X}) &= \frac{1}{Z} \prod_{R \in \mathcal{R}(G(\mathcal{X}))} \psi(\mathcal{X}_R) \\ &\propto \prod_{R \in \mathcal{R}(G(\mathcal{X}))} \tau(w_R) \\ &=: \mathcal{T}(w, G(\mathcal{X})). \end{aligned} \quad (4)$$

In other words, for a fixed (N, V, T) the density function f_X and hence the full equilibrium structure of the system is determined (pointwise) by the random field $(g(X_i))_{i \in I}$ of local descriptions $g(X_i)$ on the random graph $G(X)$.

3. Coarse local descriptions

Most practical local descriptions are not fine in the strict sense above. We therefore also consider the situation in which one has descriptions that are only approximately fine.

Let w' be a random field of non-fine or *coarse* local descriptions $w'_i = g'(X_i)$ with their σ -algebras $\sigma(w'_i) \subseteq \sigma(w_i)$, where each $w_i = g(X_i)$ is a fine local description. Then the L^2 -optimal extension of τ to coarse local description tuples $w'_R := (w'_i)_{i \in R}$ satisfies

$$\tau(w'_R) = \mathbb{E}[\psi(X_R) | \sigma(w'_R)] \quad \text{a.s.} \quad (5)$$

for every $R \in \bigcup \text{supp}(\mathcal{R}(G(X)))$, where square integrability follows from the lower bound $\Psi(\mathcal{X}_R) \geq c_R > -\infty$. That is to say, for any $\sigma(w'_R)$ -measurable square-integrable function t , one has

$$\mathbb{E}[(\psi(X_R) - \tau(w'_R))^2] \leq \mathbb{E}[(\psi(X_R) - t(w'_R))^2].$$

Consider a sequence of random fields of coarse local descriptions $w_i^{(n)}$ with their σ -algebras forming increasing filtrations $\sigma(w_i^{(n)}) \uparrow \sigma(w_i)$. We have $\sigma(w_R^{(n)}) = \bigvee_{i \in R} \sigma(w_i^{(n)})$ and hence $\sigma(w_R^{(n)}) \uparrow \sigma(w_R)$. Then

$$\tau(w_R^{(n)}) := \mathbb{E}[\psi(X_R) | \sigma(w_R^{(n)})]$$

is a martingale with respect to the filtration $\sigma(w_R^{(n)})$. By martingale convergence, for each fixed subset $R \subseteq I$,

$$\begin{aligned} \tau(w_R^{(n)}) &= \mathbb{E}[\psi(X_R) | \sigma(w_R^{(n)})] \\ &\xrightarrow[n \rightarrow \infty]{\text{a.s.}} \mathbb{E}[\psi(X_R) | \sigma(w_R)]. \end{aligned}$$

Moreover, by fineness, for every $R \in \bigcup \text{supp}(\mathcal{R}(G(X)))$, we have $\psi(X_R) = \mathbb{E}[\psi(X_R) | \sigma(w_R)]$ a.s. Since there are finitely many subsets $R \subseteq I$, and a finite union of null sets is itself null, the product over $R \in \mathcal{R}(G(X)) \subset 2^I$ converges in like manner:

$$\begin{aligned} \prod_{R \in \mathcal{R}(G(X))} \tau(w_R^{(n)}) &\xrightarrow[n \rightarrow \infty]{\text{a.s.}} \prod_{R \in \mathcal{R}(G(X))} \psi(X_R) \\ &= \exp(-\beta U(X)) \\ &= Z f_X(X). \end{aligned} \quad (6)$$

Define the normalizer

$$Z_n = \int_{\Gamma} \prod_{R \in \mathcal{R}(G(\mathcal{X}))} \tau(w_R^{(n)}) d\mathcal{X}.$$

From $\Psi(X_R) \geq c_R > -\infty$ we have $\psi(X_R) \leq \exp(-\beta c_R)$. The monotonicity of the conditional expectation gives

$$\begin{aligned} 0 &\leq \tau(w_R^{(n)}) \\ &= \mathbb{E}[\psi(X_R) | \sigma(w_R^{(n)})] \\ &\leq \exp(-\beta c_R) \quad \text{a.s.} \end{aligned}$$

It follows that

$$\prod_{R \in \mathcal{R}(G(\mathcal{X}))} \tau(w_R^{(n)}) \leq \prod_{R \in \mathcal{R}(G(\mathcal{X}))} \exp(-\beta c_R) < \infty.$$

Because on Γ we have $f_X > 0$ $d\mathcal{X}$ -a.e., any statement about X that holds a.s. also holds $d\mathcal{X}$ -a.e. on Γ .

Since $N < \infty$, the bound $\prod_{R \in \mathcal{R}(G(\mathcal{X}))} \exp(-\beta c_R) \leq \prod_{R \subseteq I} \exp(-\beta c_R)$ is uniform on Γ . And since $V < \infty$ also, the product $\prod_{R \subseteq I} \exp(-\beta c_R)$ is integrable on Γ . Then by dominated convergence and Eq. (6),

$$\begin{aligned} Z_n &= \int_{\Gamma} \prod_{R \in \mathcal{R}(G(\mathcal{X}))} \tau(w_R^{(n)}) d\mathcal{X} \\ &\xrightarrow[n \rightarrow \infty]{} \int_{\Gamma} \prod_{R \in \mathcal{R}(G(\mathcal{X}))} \psi(X_R) d\mathcal{X} \\ &= \int_{\Gamma} Z f_X(\mathcal{X}) d\mathcal{X} \\ &= Z. \end{aligned} \quad (7)$$

Combining Eqs. (6) and (7) with the strict positivity of the normalizer Z_n , we arrive at

$$\frac{1}{Z_n} \mathcal{T}(w^{(n)}, G(\mathcal{X})) \xrightarrow[n \rightarrow \infty]{d\mathcal{X}\text{-a.e.}} f_X(\mathcal{X}).$$

Thus for a fixed (N, V, T) the density function f_X and hence the full equilibrium structure is determined approximately by the random field $(g^{(n)}(X_i))_{i \in I}$ of coarse local descriptions $g^{(n)}(X_i)$ on the random graph $G(X)$.

B. Quantifying order

In the process of endowing a system with structure, interparticle interactions prevent its constituent particles from assuming statistically independent positions [30, 33, 34]. This effect, known as order, is not peculiar to crystals as the frequent interchangeable use of the terms “noncrystalline” and “disordered” might suggest but is also present in liquids and glasses, though in a much subtler form [11, 12, 29, 33, 35, 36]. In pure systems and ideal mixtures, order is strictly spatial, whereas more generally it may also be chemical [37–40]. Below we consider the degree of spatial order in the local cluster comprising a particle and its neighbors as a universal source of coarse local descriptions.

1. The degree of order

In the study of phase transitions, order parameters serve to describe the spontaneous breaking of a Hamiltonian symmetry due to the onset of a specific kind of ordering [41, 42]. By contrast, order quantification seeks to report the total degree of order in a system as evidenced by its departure from complete randomness [34, 43, 44]. Thus order quantifiers make natural order parameters, but the converse is not necessarily true.

As a first step toward making the notion of a local order quantifier precise, we introduce the degree of order Ω via an axiom that generalizes to off-lattice many-particle systems the most basic properties of absolute net magnetization per site in zero-field Ising ferromagnets [17, 45], which as illustrated in Fig. 3 is perhaps the simplest setting in which structural order can arise.

Axiom 1. For all configurations \mathcal{X} , orthogonal matrices Q , and translation vectors t ,

- (a) $\mathcal{X} \mapsto \Omega(\mathcal{X})$ (microscopicity)
- (b) $0 \leq \Omega(\mathcal{X}) < \infty$ (finite nonnegativity)
- (c) $\Omega(\mathcal{X}) = \Omega(Q\mathcal{X} + t)$ (Euclidean invariance)

Owing to the tendency of positional correlations to concentrate the configurational probability density, the degree of (dis)order in a system is closely related to its configurational entropy [46–54]. Indeed the behavior of configurational entropy in simple many-particle systems, such as bulk argon, provides a valuable macroscopic point of reference on the average microscopic degree of order. We capture this behavior in a second axiom, whenceforth we continue to write N for the number of particles, V for the volume, and T for the temperature, but now also write s for the configurational entropy per particle and $\langle \cdot \rangle$ for the ensemble average.

Axiom 2. For bulk argon in the single-phase region, away from the critical point,

- (a) $(\partial\langle\Omega\rangle/\partial s)_{N,T} < 0$ (const- T monotonicity in s)
- (b) $(\partial\langle\Omega\rangle/\partial s)_{N,V} < 0$ (const- V monotonicity in s)

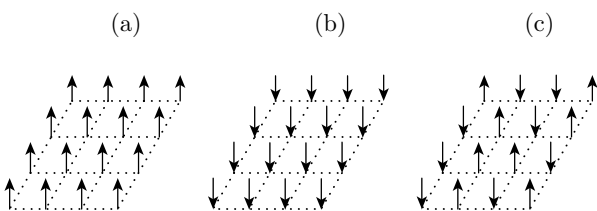


FIG. 3. Absolute net magnetization per site in a zero-field Ising ferromagnet: In its ground state, the system assumes configuration (a) or its inversion (b) with probability one, giving $|M|/N = 1$ (maximum order). Above the Curie point, each spin points in either direction with equal probability, giving $\langle|M|/N\rangle = 0$ as typified in (c), with mutually independent spins as $T \rightarrow \infty$ (complete randomness).

In sum, Axioms 1 and 2 assert that the degree of order in a many-particle system is given by a nonnegative real-valued function of the prevailing configuration with the additional properties that it is preserved under Euclidean motions and that its ensemble average in bulk argon decreases with increasing configurational entropy per particle at constant temperature or volume.

2. Local order quantifier

It is possible to regard the local cluster consisting of a central particle i and its neighbors $j \sim i$ as a system in its own right. Under this view, Axiom 1(a) implies that the degree of spatial order in a local cluster is prescribed by some function ω to be equal to $\Omega(\mathcal{X}_i)$, where \mathcal{X}_i is the restriction of the configuration \mathcal{X} to that cluster.

Let $\hat{\mathcal{V}}_i$ denote the set of all unlabeled neighbor vectors of the i th particle and consider its orbit under the action of the D -dimensional orthogonal group $O(D)$. Fix a choice of representative c and call the chosen representative $B_i = c(O(D)\hat{\mathcal{V}}_i)$ a *bond set* [55]. Then by Axiom 1(c) there exists a function Φ satisfying $\Omega(\mathcal{X}_i) = \Phi(B_i)$. From this and Axiom 1(b) it is immediate that

$$B_i \mapsto \omega(B_i), \quad 0 \leq \omega(B_i) < \infty. \quad (8)$$

We check before proceeding that $\omega(B_i)$ is a valid local description per Sec. II A 2. In representing the orthogonal orbit $O(D)\hat{\mathcal{V}}_i$ with the bond set B_i , we omit the orientations of the underlying neighbor vectors. Consequently the pair $((B_i)_{i \in I}, G)$ does not in general determine the global configuration \mathcal{X} , which implies that B_i is a local description. Thus $\omega(B_i)$, being the image of a local description, must itself be a local description.

In experiment and simulation, the microscopic character of a local cluster is frequently found to be dominated by two geometric features: the number of bonds formed by the central particle or *coordination number* k [56–66] and the angles between those bonds or *bond angles* Θ [18–20, 33, 67–73]. Following these observations, we proceed with the localization of Axiom 2(a) and (b) by studying the ensemble behaviors of k and Θ .

Let us start by considering the quasistatic compression of liquid argon at constant temperature T . The configurational entropy S of such a system decreases with an isothermal decrease in volume V at constant N , so that

$$\frac{\partial s}{\partial \rho} = \frac{1}{N} \frac{\partial S}{\partial V} \frac{\partial V}{\partial \rho} = -\frac{1}{\rho^2} \frac{\partial S}{\partial V} < 0, \quad (9)$$

where $\rho = N/V$ is the number density.

What we seek below is the direction of the concomitant change in the ensemble-average coordination number $\langle k \rangle$.

Recall that the radial distribution function (RDF) is a nonnegative function g given in the thermodynamic limit for radial distances $r > 0$ and number densities $\rho > 0$ by

$$g(r; \rho) = \lim_{\substack{N, V \rightarrow \infty \\ N/V = \rho}} \frac{V}{N(N-1)} \left\langle \sum_i \sum_{j \neq i} \frac{\delta(r - \|x_i - x_j\|)}{4\pi r^2} \right\rangle.$$

Under homogeneous and isotropic conditions such as here considered, $\langle k \rangle$ is obtained in that limit as follows:

$$\langle k \rangle = 4\pi\rho \int_0^{r_1} r^2 g(r; \rho) dr,$$

where r_1 is the ρ -dependent location of the first minimum of g . We reduce this to an integral over the unit interval by making the change of variables

$$y = r/r_1.$$

Let $Y_1 < 1$ be the reduced location of the first maximum. Define Λ as a triangular function with apex at Y_1 , left width $0 < W_L < Y_1$, and right width $W_R = 1 - Y_1$:

$$\Lambda(y) = \begin{cases} 0 & y \leq Y_1 - W_L \\ 1 - \frac{Y_1 - y}{W_L} & Y_1 - W_L < y \leq Y_1 \\ 1 - \frac{y - Y_1}{W_R} & Y_1 < y \leq Y_1 + W_R \\ 0 & y > Y_1 + W_R = 1. \end{cases}$$

Denote by $A(\rho) = g(Y_1 r_1; \rho)$ the height of the first RDF peak, which is observed empirically to satisfy

$$\frac{\partial A}{\partial \rho} > 0.$$

We may then model the first peak as

$$g_\Lambda(r; \rho) = A(\rho)\Lambda(r/r_1), \quad 0 \leq r \leq r_1,$$

and approximate the average coordination number by

$$\begin{aligned} \langle k \rangle_\Lambda(\rho) &= 4\pi\rho \int_0^{r_1} r^2 g_\Lambda(r; \rho) dr \\ &= 4\pi\rho r_1^3 \int_0^1 y^2 g_\Lambda(yr_1; \rho) dy \\ &= 4\pi\rho r_1^3 A(\rho) C, \end{aligned}$$

where

$$\begin{aligned} C &= \int_0^1 y^2 \Lambda(y) dy \\ &= \frac{W_L^3 + W_R^3}{12} + \frac{Y_1^2}{2}(W_L + W_R) + \frac{Y_1}{3}(W_R^2 - W_L^2) > 0. \end{aligned}$$

We express the difference Δ between the true average $\langle k \rangle$ and model average $\langle k \rangle_\Lambda$ in terms of the error ϵ of the peak model g_Λ with respect to the true first peak of g :

$$\begin{aligned} \Delta(\rho) &= \langle k \rangle(\rho) - \langle k \rangle_\Lambda(\rho) \\ &= 4\pi\rho \int_0^{r_1} r^2 [g(r; \rho) - A(\rho)\Lambda(r/r_1)] dr \\ &= 4\pi\rho r_1^3 \int_0^1 y^2 [g(yr_1; \rho) - A(\rho)\Lambda(y)] dy \\ &= 4\pi\rho r_1^3 A(\rho) \underbrace{\int_0^1 y^2 \left(\frac{g(yr_1; \rho)}{A(\rho)} - \Lambda(y) \right) dy}_I \\ &= 4\pi\rho r_1^3 A(\rho) \underbrace{\int_0^1 y^2 \epsilon(y; \rho) dy}_I. \end{aligned}$$

Over small changes in density, interparticle distances scale to leading order as the inverse cube root of density, so that $r_1 \approx c\rho^{-1/3}$ for some $c > 0$. Insofar as the triangle $\Lambda(y)$ agrees with the A -scaled first peak $g_\Lambda(yr_1; \rho)/A(\rho)$, the error ϵ and hence the integral I will be small. And since quasistatic changes in the density of a simple liquid result primarily in the horizontal and vertical dilation of the first RDF peak, ϵ and I will also be slow with respect to ρ , rendering $\partial I/\partial \rho$ likewise small. Thus

$$\begin{aligned} \frac{\partial \langle k \rangle}{\partial \rho} &= \frac{\partial}{\partial \rho} (\langle k \rangle_\Lambda(\rho) + \Delta(\rho)) \\ &= 4\pi \frac{\partial}{\partial \rho} (\rho r_1^3 A(\rho) (C + I)) \\ &= 4\pi \left\{ A(\rho) (C + I) \frac{\partial}{\partial \rho} (\rho r_1^3) \right. \\ &\quad \left. + \rho r_1^3 \left(\frac{\partial A}{\partial \rho} (C + I) + A(\rho) \frac{\partial I}{\partial \rho} \right) \right\} \\ &\approx 4\pi c^3 \left(\frac{\partial A}{\partial \rho} (C + I) + A(\rho) \frac{\partial I}{\partial \rho} \right) \\ &= 4\pi c^3 \left(C \frac{\partial A}{\partial \rho} + \frac{\partial A}{\partial \rho} I + A(\rho) \frac{\partial I}{\partial \rho} \right) \\ &\approx 4\pi c^3 C \frac{\partial A}{\partial \rho} \\ &> 0. \end{aligned} \tag{10}$$

Ineqs. (9) and (10) together with Axiom 2(a) imply that the ensemble-average degree of spatial order in a local cluster increases with the ensemble-average coordination number of its central particle:

$$\frac{\partial \langle \omega \rangle}{\partial \langle k \rangle} = \frac{\partial \langle \Omega \rangle}{\partial s} \frac{\partial s}{\partial \rho} \left(\frac{\partial \langle k \rangle}{\partial \rho} \right)^{-1} > 0. \tag{A}$$

Let us now consider the quasistatic heating of crystalline argon at constant volume V . In canonical equilibrium at $T > 0$ the constant-volume specific heat capacity c_V of any system with more than one energetically distinct accessible microstate satisfies

$$c_V = T \frac{\partial s}{\partial T} > 0. \tag{11}$$

Up to very high pressures, solid argon is known to have an fcc crystal structure [74]. With the coordination number of the central particle thus fixed at $k = 12$, our attention is turned to its bond angles, each belonging to one of $m = 4$ zero-temperature classes: $60^\circ, 90^\circ, 120^\circ, 180^\circ$.

Every marginal of a Gibbs measure can be written in exponential form with respect to an effective potential or potential of mean force (PMF) [75]. The partial bond angle distribution f_{Θ_i} corresponding to the i th angle class is given by

$$f_{\Theta_i}(\vartheta) = \frac{\exp(-\beta U_{\Theta_i}(\vartheta; T))}{Z_{\Theta_i}(T)},$$

where U_{Θ_i} is the PMF along the i th angular coordinate Θ_i and Z_{Θ_i} is the corresponding normalizer.

The diversity of the bond angles in each class can be assessed by the bond angle entropy $h(\Theta_i)$, evaluated as

$$\begin{aligned} h(\Theta_i) &= - \int f_{\Theta_i}(\vartheta) \ln(f_{\Theta_i}(\vartheta)) d\vartheta \\ &= - \int f_{\Theta_i}(\vartheta) [-\beta U_{\Theta_i}(\vartheta; T) - \ln(Z_{\Theta_i}(T))] d\vartheta \\ &= \beta \int U_{\Theta_i}(\vartheta; T) f_{\Theta_i}(\vartheta) d\vartheta + \ln(Z_{\Theta_i}(T)) \int f_{\Theta_i}(\vartheta) d\vartheta \\ &= \beta \langle U_{\Theta_i} \rangle + \ln(Z_{\Theta_i}(T)). \end{aligned}$$

Differentiating this with respect to temperature yields

$$\begin{aligned} \frac{\partial h(\Theta_i)}{\partial T} &= \frac{\partial h(\Theta_i)}{\partial \beta} \frac{\partial \beta}{\partial T} \\ &= \left(\beta \frac{d\langle U_{\Theta_i} \rangle}{d\beta} - \beta \left\langle \frac{\partial U_{\Theta_i}}{\partial \beta} \right\rangle \right) \left(-\frac{1}{k_B T^2} \right) \\ &= \frac{1}{k_B^2 T^3} \left(\left\langle \frac{\partial U_{\Theta_i}}{\partial \beta} \right\rangle - \frac{d\langle U_{\Theta_i} \rangle}{d\beta} \right) \\ &> 0 \end{aligned}$$

in the following two cases.

At low $T > 0$, small thermal displacements from the fcc arrangement place the crystal in the harmonic regime, in which each angular PMF is separable as $U_{\Theta}(\vartheta; T) = U_{\Theta}(\vartheta) + C(T) + \Delta(\vartheta; T)$ with $\Delta(\vartheta; T) \approx 0$ and $\partial \Delta / \partial \beta \approx 0$. We have in this case that

$$\begin{aligned} \left\langle \frac{\partial U_{\Theta}}{\partial \beta} \right\rangle - \frac{d\langle U_{\Theta} \rangle}{d\beta} &= C'(T) + \text{Var}(U_{\Theta}) - C'(T) \\ &= \text{Var}(U_{\Theta}) \\ &> 0. \end{aligned}$$

At higher T away from the melting point T_m ,

$$\begin{aligned} \left\langle \frac{\partial U_{\Theta}}{\partial \beta} \right\rangle - \frac{d\langle U_{\Theta} \rangle}{d\beta} &= \text{Var}(U_{\Theta}) + \beta \text{Cov}(U_{\Theta}, \partial_{\beta} U_{\Theta}) \\ &\geq \text{Var}(U_{\Theta}) - \beta \sqrt{\text{Var}(U_{\Theta}) \text{Var}(\partial_{\beta} U_{\Theta})} \\ &= \text{Var}(U_{\Theta}) \left(1 - \beta \sqrt{\frac{\text{Var}(\partial_{\beta} U_{\Theta})}{\text{Var}(U_{\Theta})}} \right) \\ &= \text{Var}(U_{\Theta}) \left(1 - \sqrt{\frac{\text{Var}(TS_{\Theta})}{\text{Var}(U_{\Theta})}} \right) \\ &> 0, \end{aligned}$$

where the first relation is due to the identity $d\langle U \rangle / d\beta = \langle \partial U / \partial \beta \rangle - \text{Var}(U) - \beta \text{Cov}(U, \partial_{\beta} U)$ [76]; the second follows from the Cauchy–Schwarz inequality; the third inserts $S_{\Theta} := -\partial U_{\Theta}(\vartheta; T) / \partial T$; and the fourth holds if $\text{Var}(TS_{\Theta}) < \text{Var}(U_{\Theta})$, as one is led to expect from the leading-order behaviors of U_{Θ} and TS_{Θ} ,

$$\begin{aligned} U_{\Theta}(\vartheta; T) &\approx U_{\Theta}(\vartheta_0; T) + \frac{1}{2} \kappa(\vartheta_0)(\vartheta - \vartheta_0)^2, \\ TS_{\Theta}(\vartheta; T) &\approx TS_{\Theta}(\vartheta_0; T) + \frac{k_B T}{2} \ln\left(\frac{\kappa(\vartheta)}{\kappa(\vartheta_0)}\right); \end{aligned}$$

where $\kappa(\vartheta) = \partial^2 U_{\Theta} / \partial \vartheta^2$ is the effective stiffness.

Away from T_m , the angle classes are nearly disjoint, so that the class-wise result carries over to the full bond angle distribution $f_{\Theta} := \sum_i \alpha_i f_{\Theta_i}$ with error $\epsilon(T)$:

$$\begin{aligned} \frac{\partial h(\Theta)}{\partial T} &= \frac{\partial}{\partial T} \left(\sum_{i=1}^m \alpha_i h(\Theta_i) + \sum_{i=1}^m \alpha_i \ln \alpha_i - \epsilon(T) \right) \\ &\approx \sum_{i=1}^m \alpha_i \frac{\partial h(\Theta_i)}{\partial T} \\ &> 0, \end{aligned} \tag{12}$$

where the exact equality follows from the entropy of a disjoint mixture [77, Lemma 2.5.2] and the approximate equality from $\partial \alpha_i / \partial T = 0$ (fixed class weights) and $\partial \epsilon / \partial T \approx 0$ (slowly increasing error due to class overlaps).

The combination of Axiom 2(b) with Ineqs. (11) and (12) indicates that the ensemble-average degree of spatial order in a local cluster decreases as the bond angles of the central particle become more diverse:

$$\begin{aligned} \frac{\partial \langle \omega \rangle}{\partial h(\Theta)} &= \frac{\partial \langle \Omega \rangle}{\partial s} \frac{\partial s}{\partial T} \frac{\partial T}{\partial h(\Theta)} \\ &= \frac{c_V}{T} \frac{\partial \langle \Omega \rangle}{\partial s} \left(\frac{\partial h(\Theta)}{\partial T} \right)^{-1} \\ &< 0. \end{aligned} \tag{B}$$

Ineqs. (A) and (B) recast Axiom 2(a) and (b) in terms of the ensemble behaviors of the local features k and Θ respectively. All that remains is to consider the microscopic contributions to these effects.

It can be shown that an increase in the average degree of spatial order $\langle \omega \rangle$ due to an increase in the average co-ordination number $\langle k \rangle$ is implied by an increase in the degree of spatial order ω due to an increase in the co-ordination number k :

$$\frac{\partial \omega}{\partial k} > 0 \Rightarrow \frac{\partial \langle \omega \rangle}{\partial \langle k \rangle} > 0. \tag{13}$$

It can likewise be shown that a decrease in $\langle \omega \rangle$ due to an increase in the ensemble bond angle entropy $h(\Theta)$ is implied by a decrease in ω due to an increase in the microscopic bond angle entropy $H(\theta)$, defined in Sec. III A:

$$\frac{\partial \omega}{\partial H(\theta)} < 0 \Rightarrow \frac{\partial \langle \omega \rangle}{\partial h(\Theta)} < 0. \tag{14}$$

With both Axioms 1 and 2 now expressed in local microscopic terms, we summarize the derived properties in the following definition.

Definition 3 (local order quantifier). Given a particle with bond set B , a *local order quantifier* ω is a scalar-valued function that has the following properties:

(1) $B \mapsto \omega(B)$	(local microscopicity)
(2) $0 \leq \omega(B) < \infty$	(finite nonnegativity)
(3) $\partial \omega / \partial k > 0$	(monotonicity in k)
(4) $\partial \omega / \partial H(\theta) < 0$	(monotonicity in $H(\theta)$)

Definition 3 captures in a few generic properties the geometry of spatial order in a small cluster of particles. In so doing it supplies a set of criteria for the appraisal of the local degree of order outside the setting of simple systems in thermodynamic equilibrium.

III. EXTRACOPULARITY

In view of the microscopic nature of spatial order, the study of particle positions presents itself as a logical point of departure in the search for a practical local order quantifier. In the ensuing discussion, we derive a local measure of the redundancy in neighboring particle positions and find it to be a local order quantifier in the sense of Definition 3. We then use this quantifier to establish a relationship between order and symmetry and later obtain an approximate expression for its marginal distribution in closed form.

Remark 4. Here and below the term “entropy” will refer exclusively to the information-theoretic quantity introduced by Shannon [78], which provides the information content of a data source in units of bits [77, 79]. The information-theoretic and thermostatistical notions of entropy are closely related: in the lattice formulation, Gibbs entropy is equal to the (discrete) Shannon entropy of the microstate probabilities up to a factor of $k_B \ln 2$, and in the continuum formulation, to the differential (Shannon) entropy of the phase space density up to a factor of k_B [42].

A. Parameter

For the vast majority of configurations, a complete multiset of exact pairwise distances suffices to determine the positions of $N \geq D + 2$ particles in D dimensions, up to congruence and relabeling [80, Theorem 1.6] (for a discussion on why the pair correlation function is nevertheless an incomplete invariant of structure, see Refs. 23 and 24). Such distances serve as the basis for the derivation that follows.

1. Derivation

We begin by observing that there are really only two kinds of distances in the cluster comprising a particle and its neighbors: those between the central particle and its neighbors and those among its neighbors.

Notice that each distance of the former kind corresponds to the length of a bond and each of the latter kind to the length of the difference between two distinct bonds. In a set of k bonds one has $n = \binom{k}{2}$ unordered pairs, with each bond appearing in $k - 1$ of those pairs. Thus bond pairs in fact account for both kinds of distances, so that individual bonds need not be further considered.

If all k neighbors lie in the first coordination shell, as would be the case for a conventional neighbor relation, then any differences in bond lengths will be small relative to the distances between neighbors. Indeed such differences vanish altogether in the zero-temperature limit of many common crystal structures. In this way, pairs of bonds are characterized principally by the angles they make, illustrated for a two-dimensional bond set in Fig. 4.

Let n_i denote the number of bond pairs that make the angle ϑ_i . By appeal to the original observation of Hartley [81] the information content of such a bond pair is given logarithmically by $\log_2 n_i$. We write this as follows:

$$H(\{b, b'\} | \angle\{b, b'\} = \vartheta_i) = \log_2 n_i.$$

Following Shannon’s subsequent theory [78, 82] the information content of a generic bond pair $\{b, b'\}$ after accounting for its angle $\angle\{b, b'\}$ can be written as the weighted average of the above logarithm over all m bond angle classes. The result is what one would formally describe as the conditional entropy of a bond pair given its angle,

$$\begin{aligned} H(\{b, b'\} | \angle\{b, b'\}) &= \sum_{i=1}^m \frac{n_i}{n} H(\{b, b'\} | \angle\{b, b'\} = \vartheta_i) \\ &= \frac{1}{n} \sum_{i=1}^m n_i \log_2 n_i. \end{aligned} \quad (15)$$

We term this entropy the *extracopularity parameter* \mathcal{E} .

Given a bond pair, the corresponding bond angle is uniquely determined by a simple geometric calculation. But given a bond angle, the corresponding bond pair is determined only up to the finitely many pairs that make that same angle. The greater the angular redundancy among bond pairs, the more the residual information in a generic bond pair once its angle is observed. Since a bond pair is nothing more than a pair of bonds, each giving the relative position of a neighbor of the central particle, the extracopularity parameter is precisely a measure of the angular redundancy in neighboring particle positions.

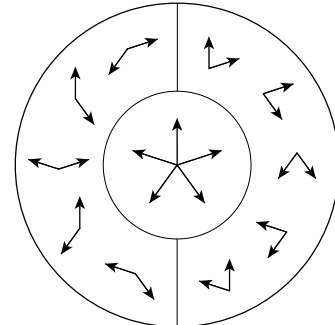


FIG. 4. A regular pentagonal bond set (center) and the partition of its bond pairs by angle: 72° (right) and 144° (left).

2. First results

Eq. (15) provides the information-theoretic definition of the extracopularity parameter \mathcal{E} . Given a tuple of bond angle multiplicities (n_1, \dots, n_m) , define the microscopic bond angle entropy $H(\theta)$ of a particle by

$$H(\theta) = - \sum_{i=1}^m \frac{n_i}{n} \log_2 \left(\frac{n_i}{n} \right), \quad n = \sum_{i=1}^m n_i. \quad (16)$$

Below we show that \mathcal{E} can be expressed also in terms of the coordination number k and the bond angle entropy $H(\theta)$.

Lemma 5. $\mathcal{E} = \log_2 \binom{k}{2} - H(\theta)$.

Proof. We have from Eq. (15) that

$$\mathcal{E} = H(\{b, b'\} \mid \angle\{b, b'\}).$$

Expanding the conditional entropy gives

$$\begin{aligned} H(\{b, b'\} \mid \angle\{b, b'\}) &= H(\angle\{b, b'\} \mid \{b, b'\}) \\ &\quad + H(\{b, b'\}) - H(\angle\{b, b'\}). \end{aligned}$$

We evaluate the terms on the right-hand side in their order of appearance. Since bond angles are uniquely determined by bond pairs,

$$H(\angle\{b, b'\} \mid \{b, b'\}) = 0.$$

A generic bond pair $\{b, b'\}$ takes one of $n = \binom{k}{2}$ values. Its Shannon entropy is therefore given by

$$\begin{aligned} H(\{b, b'\}) &= - \sum_{i=1}^m \frac{1}{n} \log_2 \left(\frac{1}{n} \right) \\ &= \log_2 n \\ &= \log_2 \binom{k}{2}. \end{aligned}$$

And the entropy of the angle between a generic pair of bonds is exactly the bond angle entropy:

$$\begin{aligned} H(\angle\{b, b'\}) &= - \sum_{i=1}^m \frac{n_i}{n} \log_2 \left(\frac{n_i}{n} \right) \\ &= H(\theta). \end{aligned}$$

From the above we obtain

$$\mathcal{E} = \log_2 \binom{k}{2} - H(\theta).$$

□

Using Lemma 5 it is easily shown that the extracopularity parameter satisfies the definition of a local order quantifier developed in Sec. II B 2. The proof of the following theorem uses the finiteness of the coordination number, itself a consequence of the finiteness of the number density.

Theorem 6. \mathcal{E} is a local order quantifier.

Proof. By Lemma 5,

$$\mathcal{E} = \log_2 \binom{k}{2} - H(\theta).$$

Property 1 of Definition 3 is then immediate given that both k and $H(\theta)$ are functions of the bond set B . We verify that \mathcal{E} possesses the remaining three properties:

Property 2.

$$H(\theta) \leq \log_2 \binom{k}{2} < \infty, \quad k < \infty.$$

Property 3.

$$\frac{\partial \mathcal{E}}{\partial k} = \frac{2k-1}{k(k-1)\ln 2} > 0, \quad k \geq 2.$$

Property 4.

$$\frac{\partial \mathcal{E}}{\partial H(\theta)} < 0, \quad k \geq 2.$$

□

Observe that the definition of \mathcal{E} by Eq. (15) leaves it undefined for $k \in \{0, 1\}$. Based on Lemma 5, property 2 of Definition 3, and its information-theoretic interpretation, we extend the parameter as follows:

$$\mathcal{E} = \begin{cases} 0 & k \in \{0, 1\} \\ \log_2 \binom{k}{2} - H(\theta) & k \in \{2, 3, \dots\}. \end{cases} \quad (17)$$

It is worthy of notice that \mathcal{E} is in a certain sense the simplest function that satisfies Definition 3. In particular, properties 3 and 4 are most easily attained by a function of additively separable form,

$$f(k, H(\theta)) = f_1(k) + f_2(H(\theta)),$$

with the unique homogeneous and isometric choice of f_2 that has property 4 being the negation function,

$$f_2(H(\theta)) = -H(\theta),$$

and the minimal choice of f_1 having property 3 being the least upper bound of the additive inverse of f_2 ,

$$f_1(k) = \log_2 \binom{k}{2},$$

which automatically ensures properties 1 and 2.

As a corollary to Theorem 6 we have that the extracopularity parameter \mathcal{E} is bounded from below by an earlier descriptor of interest called the extracopularity coefficient E [83–86], given for a particle with coordination number $k \geq 2$ and $m \leq \binom{k}{2}$ bond angle classes by

$$E = \log_2 \left(\frac{k^2 - k}{2m} \right). \quad (18)$$

Corollary 7. $\mathcal{E} \geq E$.

Proof. Since $H(\theta) \leq \log_2 m$ [79, Theorem 2.6.4],

$$\begin{aligned}\mathcal{E} &= \log_2 \binom{k}{2} - H(\theta) \\ &\geq \log_2 \binom{k}{2} - \log_2 m \\ &= \log_2 \left(\frac{k^2 - k}{2m} \right) \\ &= E.\end{aligned}$$

Evaluating Eq. (16) gives

$$\begin{aligned}H(\theta) &= - \sum_{i=1}^m \frac{n_i}{n} \log_2 \left(\frac{n_i}{n} \right) \\ &= -2 \left(\frac{30}{66} \right) \log_2 \left(\frac{30}{66} \right) - \frac{6}{66} \log_2 \left(\frac{6}{66} \right) \\ &= \log_2 11 - \frac{10}{11} \log_2 5 \\ &\approx 1.349 \text{ bits.}\end{aligned}$$

□

Table I compares the parameter \mathcal{E} with the coefficient E for a few geometries of physical prevalence. Notice that the bound provided by Corollary 7 is attained in the regular tetrahedral case, indicating that it is sharp, and that the average percentage departure of \mathcal{E} from E is under ten, suggesting that it is tight also.

We examine the regular icosahedral case, which is notable for its high symmetry [87, 88], low energy [89–91], dense packing [92, 93], and small inertia [94, 95].

Example 8. Up to a scaling and an orthogonal transformation, a regular icosahedral bond set B has the form

$$B = \{(0, \pm 1, \pm \phi), (\pm 1, \pm \phi, 0), (\pm \phi, 0, \pm 1)\},$$

where $\phi = (1 + \sqrt{5})/2$ is the golden ratio. It will be seen that B contains $k = 12$ bonds and therefore $n = 66$ bond pairs. Applying the formula

$$\angle\{b, b'\} = \arccos \left(\frac{b \cdot b'}{\|b\| \|b'\|} \right)$$

yields the following multiplicities:

$$n_i = \begin{cases} 30 & \theta_i = 63.4^\circ \\ 30 & \theta_i = 116.6^\circ \\ 6 & \theta_i = 180^\circ. \end{cases}$$

Geometry	k	$H(\theta)$	\mathcal{E}	E	$\Delta\%$
Trigonal bipyramidal	5	1.296	2.026	1.737	14.3
Regular tetrahedral	4	0.000	2.585	2.585	0.0
Pentagonal bipyramidal	7	1.705	2.688	2.392	10.1
Hexagonal bipyramidal	8	1.877	2.930	2.807	4.2
Regular octahedral	6	0.722	3.184	2.907	8.7
Square antiprismatic	8	1.379	3.429	3.222	6.0
Triangular orthobicupolar	12	2.209	3.835	3.459	9.8
Rhombic dodecahedral	14	2.455	4.053	3.923	3.3
Cuboctahedral	12	1.823	4.221	4.044	4.2
Regular icosahedral	12	1.349	4.696	4.459	5.0

Using Lemma 5 we obtain

$$\begin{aligned}\mathcal{E} &= \log_2 \binom{k}{2} - H(\theta) \\ &= \log_2 66 - \log_2 11 + \frac{10}{11} \log_2 5 \\ &= \log_2 6 + \frac{10}{11} \log_2 5 \\ &\approx 4.696 \text{ bits.}\end{aligned}$$

3. Bond angle entropy

All of the geometries so far considered are characterized by well-separated bond angles. For such geometries, the microscopic bond angle entropy $H(\theta)$ can be computed directly by inserting the associated multiplicities n_i into Eq. (16) as in Example 8. But in the generic case where one has an empirical measure of the form

$$p_\theta(\vartheta) = \frac{1}{n} \sum_{i=1}^n \delta(\vartheta - \vartheta_i), \quad (19)$$

where δ is the Dirac delta function, bond angles may not be well separated. In such situations, the multiplicities are degenerate and the usual formula cannot be used.

The naive definition of $H(\theta)$ provided by Eq. (16) can be extended to the generic case by interpolating the relationship between the (microscopic) bond angle entropy, where known, and the entropy of an embedded image of the empirical measure, which we now describe.

Before proceeding we observe that a valid assignment of bond angle entropy must come from the set of all values that can be produced by Eq. (16) for the given $k \geq 2$,

$$\begin{aligned}\mathbb{H}_k &= \left\{ - \sum_{i=1}^m \frac{n_i}{n} \log_2 \left(\frac{n_i}{n} \right) : n = \binom{k}{2}, \right. \\ &\quad \left. m \in \{1, \dots, n\}, n_i \in \mathbb{N}, \sum_{i=1}^m n_i = n \right\}. \quad (20)\end{aligned}$$

Let us write $[x]_{\mathbb{H}_k}$ for the element of \mathbb{H}_k nearest to $x \in \mathbb{R}$.

We define an embedding that convolves the empirical bond angle measure p_θ with a Gaussian kernel g_σ . This

TABLE I. Coordination number k , bond angle entropy $H(\theta)$, extracopularity parameter \mathcal{E} , extracopularity coefficient E , and the percentage departure $\Delta\%$ of the parameter from the coefficient for ten commonly encountered geometries.

produces a density on $(-\infty, +\infty)$ given by

$$\begin{aligned}(g_\sigma * p_\theta)(\vartheta) &= \frac{1}{n} \sum_{i=1}^n g_\sigma(\vartheta - \vartheta_i) \\ &= \frac{1}{n} \sum_{i=1}^n \frac{1}{\sqrt{2\pi}\sigma} \exp\left(-\frac{(\vartheta - \vartheta_i)^2}{2\sigma^2}\right).\end{aligned}$$

The embedded image entropy $\mathfrak{H}(\theta)$ is then obtained by evaluating its differential Shannon entropy:

$$\mathfrak{H}(\theta) = - \int_{-\infty}^{+\infty} (g_\sigma * p_\theta)(\vartheta) \ln[(g_\sigma * p_\theta)(\vartheta)] d\vartheta. \quad (21)$$

Consider the set \mathbb{B} of all bond sets with well-separated bond angles. It can be shown using information theory that $H(\theta)$ is approximately affine in $\mathfrak{H}(\theta)$ for such bond sets: Given a discrete random variable X with mass function p_X define $H(p_X) = H(X)$. The Shannon entropy of the Δ -quantized embedded image, $H((g_\sigma * p_\theta)_\Delta)$, satisfies

$$\begin{aligned}H((g_\sigma * p_\theta)_\Delta) &= \frac{\mathfrak{H}(\theta)}{\ln 2} + \log_2 \frac{1}{\Delta} + r_\Delta(\Delta, \sigma) \\ &= H((g_\sigma)_\Delta) + H(\theta) + r_\sigma(\Delta, \sigma),\end{aligned}$$

with $r_\Delta(\Delta, \sigma) \rightarrow 0$ as $\Delta \rightarrow 0$ by the entropy of a quantized continuous random variable [79, Theorem 8.3.1] and $r_\sigma(\Delta, \sigma) \rightarrow 0$ as $\sigma \rightarrow 0$ under well-separated bond angles by the entropy of a disjoint mixture [77, Lemma 2.5.2]. Let $\epsilon(\Delta, \sigma) = r_\Delta(\Delta, \sigma) - r_\sigma(\Delta, \sigma)$. Then

$$\begin{aligned}H(\theta) &= \frac{1}{\ln 2} \mathfrak{H}(\theta) + \log_2 \frac{1}{\Delta} - H((g_\sigma)_\Delta) + \epsilon(\Delta, \sigma) \\ &\approx c_1 \mathfrak{H}(\theta) + c_0(\Delta, \sigma), \quad c_1 = 1/\ln 2, \quad c_0(\Delta, \sigma) \in \mathbb{R}.\end{aligned}$$

Verifying this result via regression, taking \mathbb{B} to be the set of bond sets in Table I, gives an R^2 within 10^{-4} of one.

Notwithstanding this approximate affinity, a true extension of Eq. (16) must recover the exact value of $H(\theta)$ for every element of \mathbb{B} . Given a bond set $B_i \in \mathbb{B}$ denote by $H(\theta_i)$ its bond angle entropy and by $\mathfrak{H}(\theta_i)$ the entropy of the associated embedded image. We satisfy the above requirement with the following interpolation:

$$\begin{aligned}H(\theta) &= [(1-t)H(\theta_a) + tH(\theta_b)]_{\mathbb{H}_k}, \\ t &= \frac{\mathfrak{H}(\theta) - \mathfrak{H}(\theta_a)}{\mathfrak{H}(\theta_b) - \mathfrak{H}(\theta_a)};\end{aligned} \quad (22)$$

where if $\mathfrak{H}(\theta_i) \leq \mathfrak{H}(\theta) < \mathfrak{H}(\theta_j)$ for some $B_i, B_j \in \mathbb{B}$, then B_a and B_b are two bond sets in \mathbb{B} with, respectively, the largest and smallest embedded image entropies satisfying

$$\mathfrak{H}(\theta_a) \leq \mathfrak{H}(\theta) < \mathfrak{H}(\theta_b);$$

otherwise B_a and B_b are two bond sets in \mathbb{B} that minimize and maximize the embedded image entropy, respectively.

The compromise between a degenerate embedding at $\sigma = 0^\circ$ and the loss of bond angle class distinctions for σ sufficiently large suggests that the optimal embedding

scale is half the value of σ for which the two closest peaks of $g_\sigma * p_\theta$ become indistinguishable for any bond set in \mathbb{B} . For the geometries in Table I, this value is smallest in the triangular orthobicupolar case at $\sigma \approx 2.5^\circ$.

Eq. (22) has both of the two properties that would be expected of an extension of the microscopic bond angle entropy, namely that it agrees with the naive definition provided by Eq. (16) for all $B \in \mathbb{B}$ and that it is continuous with respect to the empirical measure p_θ [Eq. (19)]. Values of \mathcal{E} for geometries characterized by ill-separated (or otherwise ambiguous) bond angles, with $H(\theta)$ computed using the above extension, are given in Table II.

B. Order and symmetry

The study of the structure of many-particle systems is often concerned with symmetry, which in addition to its significance to crystals, is also important in liquids and glasses [20, 91, 96–99]. Yet the link between order and symmetry has hitherto received little attention [12, 86, 100, 101], with much of the related effort directed toward quantifying how close a local cluster is to having a certain kind of symmetry [29, 100, 102–107]. Below we establish a precise relationship between these formally distinct aspects with the help of extracopularity.

1. Point group bound

Recall from Sec. II B 2 that a bond set B is a collection of k vectors or bonds in D dimensions, where k is called the coordination number. It is helpful to introduce an idealization in which all bonds in B are equal in length.

Definition 9 (spherical). A bond set B is said to be *spherical* if it has $k > 2$ elements of the same length.

Other things being equal, a larger point group suggests a further departure from complete randomness and thus a greater degree of order. The following theorem asserts,

Geometry	k	$H(\theta)$	\mathcal{E}
Trigonal antiprismatic	6	1.519	2.388
Capped trigonal prismatic	7	1.590	2.802
Snub disphenoidal	8	1.979	2.829
Bicapped trigonal prismatic	8	1.838	2.969
Tricapped trigonal prismatic	9	1.949	3.221
Capped square antiprismatic	9	1.865	3.305
Bicapped square antiprismatic	10	2.085	3.407
Bicapped pentagonal prismatic	12	2.260	3.785
Octadecahedral	11	1.942	3.840
Capped pentagonal antiprismatic	11	1.349	4.433

TABLE II. Coordination number k , bond angle entropy $H(\theta)$, and extracopularity parameter \mathcal{E} for ten other geometries.

in accord with this intuition, that the extracopularity parameter for a spherical bond set is bounded from below by an increasing function of the size of its point group.

Theorem 10. Let B be a spherical bond set with point group G . Denote by σ_O the size of the stabilizer of a bond pair with orbit O and define $\sigma^* = \max_O \sigma_O$. Then

$$\mathcal{E} \geq E \geq \log_2 \left(\frac{|G|}{\sigma^*} \right).$$

Proof. Consider the set of all pairs of bonds in B ,

$$\binom{B}{2} = \{\{b, b'\} \subset B : b \neq b'\}.$$

The action of G on this set is defined by

$$g\{b, b'\} = \{gb, gb'\}$$

and induces a homomorphism

$$\Phi : G \rightarrow \text{Sym}(\binom{B}{2}).$$

With $k > 2$, every nontrivial element of G moves at least one bond pair. The action is therefore faithful, so that

$$|\Phi(G)| = |G|.$$

By the orbit-stabilizer theorem [108] the size of the orbit O of a bond pair with stabilizer σ_O is then given by

$$\begin{aligned} |O| &= \frac{|\Phi(G)|}{|\sigma_O|} \\ &= \frac{|G|}{|\sigma_O|}. \end{aligned} \quad (23)$$

Since the set \mathcal{O} of all $\Phi(G)$ -orbits partitions $\binom{B}{2}$, the sum of the sizes of all such orbits is equal to the total bond pair count

$$\begin{aligned} n &= \left| \binom{B}{2} \right| \\ &= \sum_{O \in \mathcal{O}} |O| \\ &= |G| \sum_{O \in \mathcal{O}} \frac{1}{|\sigma_O|}. \end{aligned} \quad (24)$$

The action of G preserves angles, and so the number m of angle classes cannot exceed the number of orbits:

$$m \leq |\mathcal{O}|. \quad (25)$$

Dividing both sides of Eq. (24) by m and then using Ineq. (25) gives

$$\begin{aligned} \frac{n}{m} &= \frac{|G|}{m} \sum_{O \in \mathcal{O}} \frac{1}{\sigma_O} \\ &\geq |G| \frac{1}{|\mathcal{O}|} \sum_{O \in \mathcal{O}} \frac{1}{\sigma_O} \\ &\geq \frac{|G|}{\sigma^*}, \end{aligned} \quad (26)$$

where the final inequality follows from the fact that $1/\sigma_O \geq 1/\sigma^*$ for all $O \in \mathcal{O}$. Now recalling Corollary 7 we arrive at

$$\begin{aligned} \mathcal{E} &\geq E \\ &= \log_2 \left(\frac{n}{m} \right) \\ &\geq \log_2 \left(\frac{|G|}{\sigma^*} \right). \end{aligned}$$

□

The second inequality in the statement of Theorem 10 can be shown to hold with equality for bond sets that have the geometry of a regular simplex or that of a regular convex polygon with an odd number of vertices. The following example demonstrates the simplicial case in three dimensions, where the bond set has a regular tetrahedral geometry.

Example 11. Let B be a regular tetrahedral bond set. We have $k = 4$ bonds, equal in length; $m = 1$ bond angle class; and $G = T_d$ as the point group, so that $|G| = 24$. The corresponding set of bond pairs takes the form

$$\binom{B}{2} = \{\{b_1, b_2\}, \{b_1, b_3\}, \{b_1, b_4\}, \{b_2, b_3\}, \{b_2, b_4\}, \{b_3, b_4\}\}.$$

Consider the stabilizer of the pair $\{b_1, b_2\}$ under the action of G . As illustrated in Fig. 5, this set has four elements: an identity

$$e : \begin{cases} \{b_1, b_2\} \mapsto \{b_1, b_2\} \\ \{b_1, b_3\} \mapsto \{b_1, b_3\} \\ \{b_1, b_4\} \mapsto \{b_1, b_4\} \\ \{b_2, b_3\} \mapsto \{b_2, b_3\} \\ \{b_2, b_4\} \mapsto \{b_2, b_4\} \\ \{b_3, b_4\} \mapsto \{b_3, b_4\} \end{cases}$$

a rotation

$$R : \begin{cases} \{b_1, b_2\} \mapsto \{b_2, b_1\} \\ \{b_1, b_3\} \mapsto \{b_2, b_4\} \\ \{b_1, b_4\} \mapsto \{b_2, b_3\} \\ \{b_2, b_3\} \mapsto \{b_1, b_4\} \\ \{b_2, b_4\} \mapsto \{b_1, b_3\} \\ \{b_3, b_4\} \mapsto \{b_4, b_3\} \end{cases}$$

and two reflections

$$M : \begin{cases} \{b_1, b_2\} \mapsto \{b_1, b_2\} \\ \{b_1, b_3\} \mapsto \{b_1, b_4\} \\ \{b_1, b_4\} \mapsto \{b_1, b_3\} \\ \{b_2, b_3\} \mapsto \{b_2, b_4\} \\ \{b_2, b_4\} \mapsto \{b_2, b_3\} \\ \{b_3, b_4\} \mapsto \{b_4, b_3\} \end{cases} \quad M' : \begin{cases} \{b_1, b_2\} \mapsto \{b_2, b_1\} \\ \{b_1, b_3\} \mapsto \{b_2, b_3\} \\ \{b_1, b_4\} \mapsto \{b_2, b_4\} \\ \{b_2, b_3\} \mapsto \{b_1, b_3\} \\ \{b_2, b_4\} \mapsto \{b_1, b_4\} \\ \{b_3, b_4\} \mapsto \{b_3, b_4\} \end{cases}$$

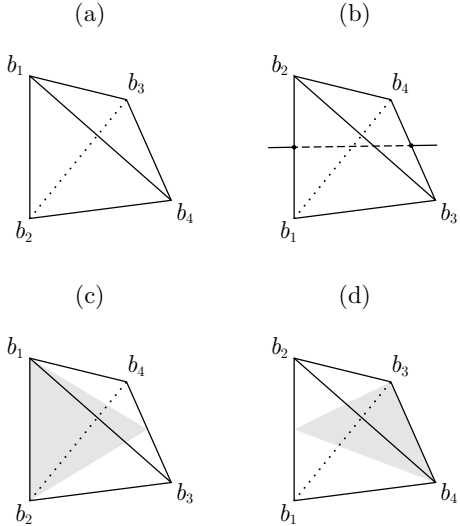


FIG. 5. The stabilizer of the bond pair $\{b_1, b_2\}$ under the action of the tetrahedral point group T_d : (a) the identity e , (b) the rotation R , (c) the reflection M , and (b) the reflection M' . Here bonds are represented not by arrows as is usually done but by the vertices at their terminal points, so that bond pairs correspond to the line segments joining those vertices.

By the edge-transitivity of the regular tetrahedron, all $n = 6$ pairs in $\binom{B}{2}$ have the same orbit and therefore stabilizers of the same size $\sigma^* = \max\{4\} = 4$. Thus

$$\begin{aligned} \mathcal{E} &= E \\ &= \log_2\left(\frac{n}{m}\right) \\ &= \log_2\left(\frac{4n}{4m}\right) \\ &= \log_2\left(\frac{|G|}{\sigma^*}\right). \end{aligned}$$

2. Icosahedral maximum

The regular icosahedron has the largest point group among all convex polyhedra with a vertex count of at most 12, this being the kissing number in three dimensions [109, 110]. We now prove an analogous result for the lower bound E of the extracopularity parameter.

Proposition 12. Let B be a spherical bond set in \mathbb{R}^3 with coordination number $k = |B| \leq 12$. Then $E \leq E_{\text{ico}}$.

Proof. Let $E = E(k, m)$. A regular icosahedral bond set places $k = 12$ points on a sphere with $m = 3$ distinct central angles. Using Eq. (18) we have $E_{\text{ico}} = E(12, 3) = \log_2(22)$. We show that no valid combination of k and m gives higher E . Since E is strictly increasing in k , it suffices to check the largest admissible k for each m . And since E is strictly decreasing in m , we need not check $m > 3$. For $m = 3$, we have $E(k, 3) \leq E(12, 3)$ by the

hypothesis that $k \leq 12$. For $m = 2$, no more than $k = 6$ points can be placed on a sphere [111, Theorem 2]; hence $E(k, 2) \leq E(6, 2) = \log_2(15/2) < \log_2(22) = E(12, 3)$. For $m = 1$, no more than $k = 4$ points can be placed on a sphere; hence $E(k, 1) \leq E(4, 1) = \log_2(6) < \log_2(22) = E(12, 3)$. Thus $E \leq E(12, 3) = E_{\text{ico}}$. \square

C. Distribution function

By Theorem 6, the extracopularity parameter \mathcal{E} is a local order quantifier in the sense of Definition 3 and hence a source of coarse local descriptions as defined in Sec. II A 3. Accordingly some function of the values of \mathcal{E} for all particles in a system approximates a complete invariant for its structure. In many cases, however, the statistical behavior of a local descriptor for a single particle suffices to draw distinctions between structures. We therefore focus the subsequent discussion on the marginal distribution of \mathcal{E} .

Define the *extracopularity distribution function* (XDF) $p_{\mathcal{E}}$ as the marginal probability mass function of the extracopularity parameter for a given particle. We may write the conditional distribution of \mathcal{E} given k piecewise.

$$P\{\mathcal{E} = \varepsilon \mid k = \kappa\} = \begin{cases} \mathbf{1}\{\varepsilon = 0\} & \kappa \in \{0, 1, 2\} \\ P\{\log_2\binom{k}{2} - H(\theta) = \varepsilon \mid k = \kappa\} & \kappa \in \{3, 4, \dots\}, \end{cases}$$

where $\mathbf{1}\{A\}$ denotes the indicator function of the condition A . The XDF can then be expressed as a mixture of the following form:

$$\begin{aligned} p_{\mathcal{E}}(\varepsilon) &= P\{\mathcal{E} = \varepsilon\} \\ &= \sum_{\kappa=0}^{\infty} p_k(\kappa) P\{\mathcal{E} = \varepsilon \mid k = \kappa\} \\ &= (p_k(0) + p_k(1) + p_k(2)) \mathbf{1}\{\varepsilon = 0\} \\ &\quad + \sum_{\kappa=3}^{\infty} p_k(\kappa) P\{H(\theta) = \log_2\binom{k}{2} - \varepsilon \mid k = \kappa\}. \end{aligned} \quad (27)$$

The second factor of each term in the series is determined by the conditional distribution of the microscopic bond angle entropy $H(\theta)$ given the coordination number k . Below this function is approximated for particles with high coordination numbers and broad bond angle distributions.

Recall from Sec. III A 3 that the (microscopic) bond angle entropy $H(\theta)$ is a functional of the empirical bond angle measure p_{θ} . This measure is itself a function of a sample from the ensemble bond angle distribution f_{θ} , given for a tuple of $\nu = \binom{\kappa}{2}$ angles $(\Theta^{(1)}, \dots, \Theta^{(\nu)})$ by

$$f_{\Theta}(\vartheta^{(1)}, \dots, \vartheta^{(\nu)}) = \frac{1}{\nu!} \left\langle \sum_{\pi \in \text{Sym}(\{1, \dots, \nu\})} \prod_{j=1}^{\nu} \delta(\Theta^{\pi(j)} - \vartheta^{(j)}) \right\rangle. \quad (28)$$

Hence the bond angle entropy as it is formally extended in Eq. (22) is better suited to numerical evaluation.

In order to proceed symbolically, one may work with a tractable estimator of $H(\theta)$. We start by partitioning the bond angle interval $(0^\circ, 180^\circ]$ into M equal-width bins

$$I_i = \left(\frac{180^\circ}{M}(i-1), \frac{180^\circ}{M}i \right], \quad i = 1, \dots, M.$$

Let \hat{n}_i denote the number of bond pairs whose angles lie in the i th bin, so that $\sum_{i=1}^M \hat{n}_i = \nu$. Then $(\hat{n}_1, \dots, \hat{n}_M)$ is an M -bin bond angle histogram and the corresponding maximum likelihood estimator of the bond angle entropy takes the form

$$\hat{H}(\theta) = - \sum_{i=1}^M \frac{\hat{n}_i}{\nu} \log_2 \left(\frac{\hat{n}_i}{\nu} \right). \quad (29)$$

We suppose that each histogram is constructed from ν independent samples from the discretized one-angle marginal p_{Θ} , defined for the M bin centers ϑ_i by

$$p_{\Theta}(\vartheta_i) = \int_{(0^\circ, 180^\circ]^{\nu-1}} \int_{I_i} f_{\Theta}(\vartheta', \vartheta^{(2)}, \dots, \vartheta^{(\nu)}) d\vartheta' d^{\nu-1}\vartheta. \quad (30)$$

Under this simplifying assumption we have multinomial histogram probabilities

$$P\{\hat{n}_1 = \nu_1, \dots, \hat{n}_M = \nu_M\} = \frac{\nu!}{\nu_1! \dots \nu_M!} \prod_{i=1}^M p_{\Theta}(\vartheta_i)^{\nu_i}.$$

The conditional probabilities of the bond angle entropy estimates are then given by

$$\begin{aligned} P\{\hat{H}(\theta) = \mathcal{H} \mid k = \kappa\} &= P\{\hat{H}(\theta) = \mathcal{H} \mid n = \nu\} \\ &= \sum_{\substack{(\nu_1, \dots, \nu_M): \\ \hat{H}(\theta) = \mathcal{H}}} \nu! \prod_{i=1}^M \frac{p_{\Theta}(\vartheta_i)^{\nu_i}}{\nu_i!}. \end{aligned}$$

For large ν and comparable $p_{\Theta}(\vartheta_i)$ the foregoing may be approximated by a normal distribution

$$\mathcal{N}[\mu_{\hat{H}(\theta)|k}(\kappa), \sigma_{\hat{H}(\theta)|k}^2(\kappa)] \quad (31)$$

with mean $\mu_{\hat{H}(\theta)|k}(\kappa)$ and variance $\sigma_{\hat{H}(\theta)|k}^2(\kappa)$.

The mean is obtained by subtracting the bias term from the first-order expectation expansion [112, 113]:

$$\mu_{\hat{H}(\theta)|k}(\kappa) \approx - \sum_{i=1}^M p_{\Theta}(\vartheta_i) \log_2 p_{\Theta}(\vartheta_i) - \frac{m-1}{2(\kappa) \ln 2}, \quad (32)$$

where $m \leq M$ is the number of nonempty bins and $0 \log_2 0 = 0$ by convention.

The variance is in turn obtained using the delta method [114], which linearizes the entropy functional via a first-order Taylor expansion:

$$\begin{aligned} \sigma_{\hat{H}(\theta)|k}^2(\kappa) &\approx \frac{1}{(\kappa)} \left\{ \sum_{i=1}^M p_{\Theta}(\vartheta_i) \left(\log_2 p_{\Theta}(\vartheta_i) + \frac{1}{\ln 2} \right)^2 \right. \\ &\quad \left. - \left[\sum_{i=1}^M p_{\Theta}(\vartheta_i) \left(\log_2 p_{\Theta}(\vartheta_i) + \frac{1}{\ln 2} \right) \right]^2 \right\}. \end{aligned} \quad (33)$$

Together Eqs. (27) and (29)–(31) produce a formula for the XDF of a highly coordinated particle with broadly distributed bond angles:

$$\begin{aligned} Z_{\mathcal{E}p_{\mathcal{E}}}(\varepsilon) &\approx \mathbf{1}\{\varepsilon = 0\} \sum_{\kappa=0}^2 p_k(\kappa) + \sum_{\kappa=3}^K p_k(\kappa) \\ &\quad \frac{1}{\sigma_{\hat{H}(\theta)|k}(\kappa)} \exp \left\{ -\frac{1}{2} \left(\frac{\log_2(\kappa) - \varepsilon - \mu_{\hat{H}(\theta)|k}(\kappa)}{\sigma_{\hat{H}(\theta)|k}(\kappa)} \right)^2 \right\}, \\ \varepsilon &\in \left\{ \log_2 \left(\frac{a}{2} \right) - b : a \in \mathbb{N}, 2 \leq a \leq K, b \in \mathbb{H}_a \right\}; \end{aligned} \quad (34)$$

with the series in Eq. (27) here truncated at some $K \gg 3$.

Eq. (34) is in essence a Gaussian mixture with mixture weights $p_k(\kappa)$, component means

$$\mu_{\mathcal{E}|k}(\kappa) = \begin{cases} 0 & \kappa \in \{0, 1\} \\ \log_2(\kappa) - \mu_{\hat{H}(\theta)|k}(\kappa) & \kappa \in \{2, 3, \dots\}, \end{cases}$$

and component variances

$$\sigma_{\mathcal{E}|k}^2(\kappa) = \sigma_{\hat{H}(\theta)|k}^2(\kappa), \quad \kappa \in \{2, 3, \dots\}.$$

Using the laws of total expectation and variance its first two moments reduce respectively to

$$\begin{aligned} \mu_{\mathcal{E}} &= \sum_{\kappa=3}^K p_k(\kappa) [\log_2(\kappa) - \mu_{\hat{H}(\theta)|k}(\kappa)], \\ \sigma_{\mathcal{E}}^2 &= \sum_{\kappa=3}^K p_k(\kappa) \sigma_{\hat{H}(\theta)|k}^2(\kappa) + \sum_{\kappa=0}^2 p_k(\kappa) (0 - \mu_{\mathcal{E}})^2 \\ &\quad + \sum_{\kappa=3}^K p_k(\kappa) [\log_2(\kappa) - \mu_{\hat{H}(\theta)|k}(\kappa) - \mu_{\mathcal{E}}]^2. \end{aligned}$$

It may be noted that the first summation in the expression for variance corresponds to the within-component and the sum of the second two to the between-component contributions to the total variance. Higher moments of the XDF can be computed in like manner.

IV. ELEMENTARY MATERIALS

Certain of the many possible forms of matter occupy a place of special importance in our theoretical understanding of structure in many-particle systems. In what

follows we use the distribution function introduced above to study the structure of the most elementary manifestations of the three conventional states of matter: the ideal gas, the perfect crystal, and the simple liquid.

A. Ideal gas

The usual starting point for discussing structure in particle systems is the bulk ideal gas, wherein the absence of interactions and the negligibility of boundaries result in a trivial behavior that nonetheless proves instructive.

Let us begin by considering the distribution of the angle between the neighbor vectors of an ideal gas particle. Vectors of this kind are analogous to bonds in systems with interactions and will therefore be referred to as such.

Absent interactions and boundaries, individual bonds exhibit no preference for any particular direction in space. However, as seen in Fig. 6(a), fixing one bond b renders the probability of observing the second bond b' at an angle $\Theta \leq \vartheta$ from b proportional to the spherical cap surface area

$$A_\vartheta = 2\pi r^2(1 - \cos \vartheta).$$

Normalizing A_ϑ by the total area of the sphere gives the cumulative probability

$$\begin{aligned} P\{\Theta \leq \vartheta\} &= \frac{A_\vartheta}{4\pi r^2} \\ &= \frac{1 - \cos 2\vartheta}{2}. \end{aligned}$$

Differentiating the above expression yields the ensemble bond angle distribution for the bulk ideal gas:

$$\begin{aligned} f_\Theta(\vartheta) &= \frac{d}{d\vartheta} P\{\Theta \leq \vartheta\} \\ &= \frac{1}{2} \sin \vartheta, \quad 0^\circ < \vartheta \leq 180^\circ. \end{aligned} \quad (35)$$

Fig. 6(b) illustrates this distribution.

We now turn to the coordination number k . Recall that an ideal gas of density ρ can be regarded as the

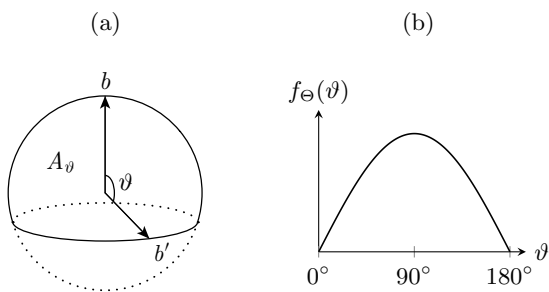


FIG. 6. (a) In an ideal gas, the probability of two notional bonds b and b' making an angle $\Theta \leq \vartheta$ is proportional to the spherical cap area A_ϑ . (b) The ensemble bond angle distribution of an ideal gas particle is given by a sine function.

point-particle limit of a hard-sphere fluid with that same density. Indeed as the particle radius r_0 approaches zero the hard-sphere fluid converges to a homogeneous Poisson point process [34], for which the probability of finding N particles in a region of volume V is equal to

$$\frac{(\rho V)^N}{N!} \exp(-\rho V).$$

It is an empirical observation that the location r_1 of the first RDF minimum and the particle radius r_0 satisfy the inequality $r_1 \leq 4r_0$ across packing fractions in three-dimensional hard-sphere fluids [115–117]. Let K be the number of particles within a radial distance of $4r_0$. Then

$$\begin{aligned} P\{k \geq 2\} &\leq P\{K \geq 2\} \\ &\xrightarrow[r_0 \rightarrow 0]{} 1 - (1 + \rho |B(4r_0)|) \exp(-\rho |B(4r_0)|) \\ &= 0, \end{aligned}$$

where $|B(r)|$ denotes the volume of a ball with radius r . It follows that

$$\begin{aligned} P\{\mathcal{E} = 0\} &\geq P\{k < 2\} \\ &= 1 - P\{k \geq 2\} \\ &\xrightarrow[r_0 \rightarrow 0]{} 1. \end{aligned}$$

Thus the behavior of k by itself implies that the XDF of an ideal gas particle is a single point mass at zero:

$$p_{\mathcal{E}}(\varepsilon) = \begin{cases} 1 & \varepsilon = 0 \\ 0 & \varepsilon > 0. \end{cases} \quad (36)$$

This is consistent with the traditional understanding that the ideal gas is completely devoid of order and structure.

B. Perfect crystal

Often held in contrast with the ideal gas is the perfect crystal, in which strong interparticle interactions give rise to a periodic arrangement of equilibrium positions about which particles undergo thermal motion. At zero temperature [118], a perfect crystal with one crystallographically independent site will have an XDF that is degenerate at a certain value \mathcal{E}_0 . Below we calculate this value for six such crystals, consider the qualitative behavior of the first two XDF moments at positive temperatures, and briefly discuss the treatment of temperature gradients.

1. Zero temperature

The dense configuration that results from the stacking of hexagonal layers in an ABC sequence is the face-centered cubic (fcc) crystal structure. Such a structure attains the maximum packing fraction φ [119] and the largest point group G of any periodic arrangement in Euclidean 3-space [120]. Its \mathcal{E}_0 is calculated at 4.221 bits.

By instead stacking hexagonal layers in a truncated AB sequence, one obtains the hexagonal close-packed (hcp) crystal structure. Hcp is equal in packing fraction to fcc but has a point group that is only half as large. Repeating the calculation for hcp, it is found that the latter distinction is reflected in a smaller \mathcal{E}_0 of 3.835 bits.

If in addition to truncating the stacking sequence to AB, one uses square rather than hexagonal layers, a body-centered cubic (bcc) crystal structure is obtained. Bcc has the same octahedral point group as fcc but packs particles less efficiently. Evaluating the parameter for bcc, taking $k = 14$ as most often done [115, 121–124], we find that a lower packing fraction is likewise reflected in a smaller \mathcal{E}_0 as compared to fcc at 4.053 bits.

Stacking square layers in the trivial AA sequence gives rise to a simple cubic (sc) crystal structure. Sc also possesses the octahedral point symmetry seen in fcc and bcc but has the lowest packing fraction of the three structures. This additional reduction in packing efficiency is observed to produce a still smaller \mathcal{E}_0 of 3.185 bits.

Table III compares the above four crystal structures and two others. Across all pairs of structures it is observed that every increase in \mathcal{E}_0 is explained by a corresponding increase in packing fraction or point group order. By contrast the widely used Steinhardt rotational invariant q_6 [29] lacks this property for five of those pairs, namely (α-As, sc), (dc, sc), (dc, hcp), (dc, bcc), and (dc, fcc). It is noteworthy that the related invariants q_4 and w_6 are found upon further examination to be so afflicted in at least as many instances.

The results of Sec. II B suggest that the local degree of order grows with an increase or control of the bond count k and a control or decrease of the bond angle entropy $H(\theta)$. The interplay between more bonding and less bond angle diversity can be made explicit by rewriting the formula of Lemma 5 so that k and $H(\theta)$ appear in separate factors:

$$\mathcal{E} = \log_2 \left(\binom{k}{2} 2^{-H(\theta)} \right). \quad (37)$$

In so doing we recast \mathcal{E} as the logarithm of the area of a rectangle with height $\binom{k}{2}$ and width $2^{-H(\theta)}$. Fig. 7 illustrates this geometric interpretation for five of the crystal structures in Table III.

Crystal structure	φ	$ G $	q_6	k	$H(\theta)$	\mathcal{E}_0
Rhombohedral (α-As)	0.39	12	0.42	6	1.371	2.536
Diamond cubic (dc)	0.34	24	0.62	3	0.000	2.585
Simple cubic (sc)	0.52	48	0.35	6	0.722	3.185
Hexagonal close-packed (hcp)	0.74	24	0.49	12	2.209	3.835
Body-centered cubic (bcc)	0.68	48	0.50	14	2.455	4.053
Face-centered cubic (fcc)	0.74	48	0.57	12	1.823	4.221

TABLE III. The packing fraction φ , point group order $|G|$, rotational invariant q_6 , coordination number k , bond angle entropy $H(\theta)$, and extracopularity value \mathcal{E}_0 for six crystal structures with one crystallographically independent site.

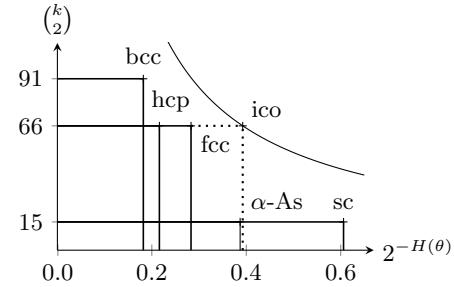


FIG. 7. The extracopularity parameter, interpreted geometrically as the logarithm of the area of a rectangle. Crystal structures are compared to the icosahedral value and its “isoextracopularity” curve. The rectangle for dc is omitted, as it exceeds the depicted range, with its upper right vertex at (1, 6).

A perfect icosahedral crystal, while incompatible with translational symmetry in Euclidean space, can nevertheless be realized in a space of constant positive curvature [125, 126]. The optimality of icosahedral clusters in symmetry, energy, and packing leads us to ask whether a crystal composed of such clusters would have the largest \mathcal{E}_0 . We capture the implied frontier by setting Eq. (37) equal to the value of \mathcal{E} obtained in Example 8. This produces the hyperbola seen in Fig. 7 and given as follows:

$$\binom{k}{2} 2^{-H(\theta)} = 6 \cdot 5^{10/11}, \quad k \geq 2, \quad H(\theta) \geq 0. \quad (38)$$

By Proposition 12 the sharp lower bound E of the parameter \mathcal{E} is maximized by the regular icosahedral geometry for spherical bond sets in $D = 3$ with $k \leq 12$. And in Table I we see that E and \mathcal{E} induce identical orderings for the geometries therein considered. It is therefore reasonable to conjecture that \mathcal{E} too is maximized by the icosahedral arrangement under those same conditions.

2. Positive temperatures

On account of thermal motion, even a perfect crystal with a single crystallographically independent site will exhibit nonzero variation in \mathcal{E} at positive temperature. Since in any such crystal each atom has a constant $k \geq 2$, the XDF simplifies to

$$p_{\mathcal{E}}(\varepsilon) = P\{H(\theta) = \log_2 \binom{k}{2} - \varepsilon\}.$$

Using Lemma 5 and Bienaymé’s identity gives

$$\begin{aligned} \text{Var}(\mathcal{E}) &= \text{Var}(\log_2 \binom{k}{2}) + \text{Var}(H(\theta)) \\ &\quad - 2 \text{Cov}(\log_2 \binom{k}{2}, H(\theta)) \\ &= \text{Var}(H(\theta)). \end{aligned}$$

It is now readily seen that for $T > 0$,

$$\begin{aligned} \text{Var}(\mathcal{E}_T) &= \text{Var}(H(\theta_T)) \\ &> 0 \\ &= \text{Var}(H(\theta_0)) \\ &= \text{Var}(\mathcal{E}_0). \end{aligned} \quad (39)$$

One expects to see the opposite behavior in the mean. It follows from Lemma 5 and the linearity of the expected value that

$$\langle \mathcal{E} \rangle = \langle \log_2 \binom{k}{2} \rangle - \langle H(\theta) \rangle. \quad (40)$$

We expand the ensemble average of the microscopic bond angle entropy as follows:

$$\langle H(\theta) \rangle = H(\Theta) - \frac{m-1}{2 \binom{k}{2} \ln 2} - \chi(k, m, f_\Theta),$$

where the first term is the entropy of the discretized ensemble bond angle distribution [Eq. (30)], the second is the first-order bias correction under independent angles [112], and the third encompasses higher-order corrections for bias and angle dependence per Eq. (28). For a uniform M -bin discretization one has

$$H(\Theta) = \frac{h(\Theta)}{\ln 2} + \log_2 \frac{180^\circ}{M} + o(1).$$

Call the remainder

$$r = H(\Theta) - \left(\frac{h(\Theta)}{\ln 2} + \log_2 \frac{180^\circ}{M} \right).$$

Inserting the above into Eq. (40) and differentiating the result with respect to temperature yields

$$\frac{\partial \langle \mathcal{E} \rangle}{\partial T} = -\frac{1}{\ln 2} \frac{\partial h(\Theta)}{\partial T} - \frac{\partial r}{\partial T} + \frac{\partial \chi}{\partial T}, \quad (41)$$

where we have used the fact that k , m , and M are here constant. A crystalline bond angle distribution consists of finitely many peaks broadening slowly with temperature, so that

$$\frac{\partial r}{\partial T} \approx 0 \quad \text{and} \quad \frac{\partial \chi}{\partial T} \approx 0.$$

Applying these and recalling Ineq. (12) yields

$$\frac{\partial \langle \mathcal{E} \rangle}{\partial T} \approx -\frac{1}{\ln 2} \frac{\partial h(\Theta)}{\partial T} < 0, \quad (42)$$

which agrees with our intuition.

3. Temperature gradient

Crystals as well as solids of other kinds are often out of thermal and indeed thermodynamic equilibrium. To facilitate the study of structure in nonequilibrium states we may write the extracopularity parameter as a scalar field $x \mapsto \mathcal{E}(x)$ defined by

$$\mathcal{E}(x) = \sum_{i=1}^N \mathcal{E}_i \delta(x - x_i).$$

The spatial variation in the local degree of order at a specified length scale σ can then be resolved by coarse-graining the microscopic field \mathcal{E} through its convolution with the D -dimensional Gaussian kernel

$$g_\sigma(x) = \frac{1}{(2\pi\sigma^2)^{D/2}} \exp\left(-\frac{|x|^2}{2\sigma^2}\right).$$

The resulting coarse-grained field is given by

$$\begin{aligned} \mathcal{E}_\sigma(x) &= (g_\sigma * \mathcal{E})(x) \\ &= \int g_\sigma(x - x') \mathcal{E}(x') dx' \\ &= \sum_{i=1}^N \mathcal{E}_i g_\sigma(x - x_i). \end{aligned}$$

An example of this field at the scale of the lattice constant is provided in Fig. 8.

C. Simple liquid

The study of the structure of matter in the liquid state is made difficult by the fact such systems admit neither the idealization of independent particle positions nor that of periodic particle arrangement. To address this difficulty, various notions of a “simple liquid” have been put forward [16, 127, 128], all centering on a homogeneous condensed fluid with isotropic interactions. In the discussion that follows we consider bulk liquid argon near its triple point, which has long been recognized to exemplify that description.

1. Coordination process

We begin by conceiving of coordination as a local process in which nearby atoms compete to lie within the vicinity of a reference particle. Regarding this process

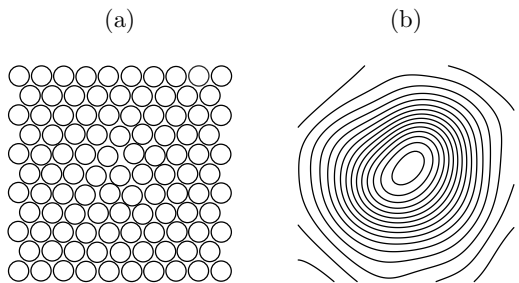


FIG. 8. Extracopularity field in two dimensions: (a) a hexagonal crystal with a negative radial temperature gradient, decreasing outward from $T_1 \approx T_m$ at the center to $T_2 \approx 0$ at the boundary of the square region; (b) the coarse-grained extracopularity field \mathcal{E}_σ with scale σ equal to the lattice constant, decreasing inward from the zero-temperature value of $\mathcal{E}_0 \approx 2.385$ bits at the boundary in increments of 0.05 bits.

as sampling without replacement is equivalent to modeling the coordination number k to be hypergeometrically distributed:

$$\hat{p}_k(\kappa; \Lambda, \lambda, K) = \frac{\binom{\lambda}{\kappa} \binom{\Lambda-\lambda}{K-\kappa}}{\binom{\Lambda}{K}},$$

$$\max\{0, K + \lambda - \Lambda\} \leq \kappa \leq \min\{K, \lambda\}; \quad (43)$$

where the Λ (population size), λ (number of possible successes), and K (number of draws) are positive integers satisfying $\lambda \leq \Lambda$ and $K \leq \Lambda$ [129]. Each of these parameters has a clear physical interpretation in the present setting aside from K , which we later obtain by using the first moment formula

$$\mu_k = \mathbb{E}[k]$$

$$= \frac{\lambda}{\Lambda} K. \quad (44)$$

The number λ of possible successes captures the probabilistic upper bound imposed on the coordination number by packing constraints. For the purposes of determining its value we treat atoms as hard spheres.

Let r_0 be half the radial distance to the first RDF maximum (particle radius), r_1 the radial distance to the first RDF minimum (interaction radius), and r_2 that to its second minimum (outer boundary), each illustrated in Fig. 9(a). Then the volume of the vicinity may be approximated as

$$V = \frac{4}{3}\pi(r_1^3 - r_0^3)$$

$$\approx \frac{4}{3}\pi[(3r_0)^3 - r_0^3]$$

$$= \frac{104}{3}\pi r_0^3.$$

The maximum packing fraction of an irregular arrangement of identical hard spheres is widely reported to be $\varphi \approx 0.64$ [65, 115, 130, 131]. The value of λ implied by this fraction is determined, up to rounding, by the ratio of the volume of all atoms that lie in the vicinity to that of a single such atom:

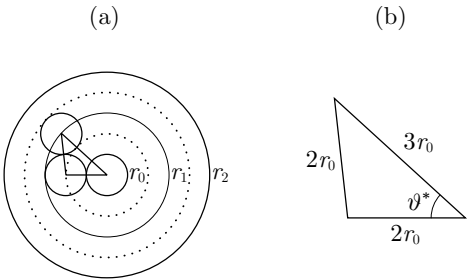


FIG. 9. Atomic vicinity in the hard-sphere treatment: (a) the boundaries of key regions; (b) the geometry of the minimum bond angle configuration of an atom and two of its neighbors.

$$\lambda = \left\lfloor \frac{\varphi V}{(4/3)\pi r_0^3} \right\rfloor = 17, \quad (45)$$

where $\lfloor x \rfloor$ denotes the integer nearest to x .

The first moment μ_k corresponds to the average number of atoms within the interaction radius r_1 . We take the population size Λ to be that number within the outer boundary r_2 . At a temperature of 85 K and a pressure of 1 atm [16, 132, 133] this gives

$$\mu_k = 4\pi\rho \int_{r_0}^{r_1} r^2 g(r) dr \approx 12.2, \quad (46)$$

$$\Lambda = 4\pi\rho \int_{r_0}^{r_2} r^2 g(r) dr \approx 54.$$

These two values coincide to the nearest integer with the numbers of atoms in the first and first two shells of the Mackay icosahedral cluster, respectively [134–136].

Now solving Eq. (44) for K with λ , μ_k , and Λ as given above we obtain

$$K = \left\lfloor \frac{\Lambda}{\lambda} \mu_k \right\rfloor = 39. \quad (47)$$

Inserting Eqs. (45)–(47) into Eq. (43) produces the following model of the coordination number distribution:

$$\hat{p}_k(\kappa) = \begin{cases} \frac{\binom{17}{\kappa} \binom{37}{39-\kappa}}{\binom{54}{39}} & 2 \leq \kappa \leq 17 \\ 0 & \text{otherwise.} \end{cases} \quad (48)$$

2. Bond angle model

Liquid argon is distinguished from an ideal gas of the same number density primarily by the presence of strong repulsive forces [137]. Such forces discourage small interatomic distances, thereby suppressing the occurrence of sharp angles. A basic model of the ensemble bond angle distribution may therefore be derived by truncating the ideal gas solution in Eq. (35) as follows:

$$\hat{p}_\Theta(\vartheta_i) = \begin{cases} 0 & \vartheta_i < \vartheta^* \\ \sin \vartheta_i / \hat{Z}_\Theta & \vartheta_i \geq \vartheta^*, \end{cases} \quad (49)$$

where ϑ^* is a cutoff angle, \hat{Z}_Θ is the normalizer, and the bin-center angles ϑ_i are given for integers $1 \leq i \leq M$ by

$$\vartheta_i = 180^\circ \left(\frac{2i-1}{2M} \right). \quad (50)$$

The cutoff angle ϑ^* is determined by appealing to the hard-sphere treatment a second time. As illustrated in Fig. 9(a) and (b), hard spheres produce the smallest attainable bond angle when the central atom combines with two other atoms within a distance of r_1 to form an isosceles triangle of side lengths $a = b = 2r_0$ and $c = 3r_0$. By

elementary trigonometry the cosine of its obtuse angle is computed as

$$\frac{a^2 + b^2 - c^2}{2ab} = -\frac{1}{8}.$$

Solving for the acute angle yields

$$\vartheta^* = \frac{180^\circ - \arccos(1/8)}{2} \approx 41.41^\circ. \quad (51)$$

Fig. 10 depicts the truncation at this angle.

We determine the number M of bins by considering the scale of bond angle fluctuations. Recall that the Lindemann parameter L gives the root-mean-square value of atomic displacements relative to the nearest-neighbor distance at the melting point [138, 139]. The corresponding bond angle fluctuations are hence of order

$$\begin{aligned} \Delta\theta &= \sqrt{L^2 + L^2} \\ &= \sqrt{2}L \text{ rad.} \end{aligned}$$

It will be seen that $\Delta\theta$ serves as a lower bound on the scale of those same fluctuations in liquid state. Requiring the width of each bin to equal $\Delta\theta$ is therefore tantamount to ensuring that the typical fluctuation of the average bond angle class is registered. This requirement is captured by the function

$$F : L \mapsto \frac{\pi}{\sqrt{2}L}.$$

Reported values of L lie in the range 0.10–0.15 [140–142]. We assign to M the integer closest to the average of the values of F at the minimum and maximum of this range:

$$M = \left\lceil \frac{F(0.10) + F(0.15)}{2} \right\rceil = 19. \quad (52)$$

Using Eq. (52) in Eq. (50) it is found that the inequality $\vartheta_i \geq \vartheta^* \approx 41.41^\circ$ is satisfied for indexes $i \geq 5$. The resulting bond angle model is given in closed form by

$$\begin{aligned} \hat{p}_\Theta(\vartheta_i) &= \frac{1}{\hat{Z}_\Theta} \sin \vartheta_i, \\ \hat{Z}_\Theta &= \sum_{i=5}^{19} \sin \vartheta_i \approx 10.832; \\ \vartheta_i &= 180^\circ \left(\frac{2i-1}{38} \right), \\ i &= 5, 6, \dots, 19. \end{aligned} \quad (53)$$

3. XDF

Combining the formula obtained in Sec. III C with the models of the coordination number and bond angle distribution developed in Secs. IV C 1 and IV C 2 respectively,

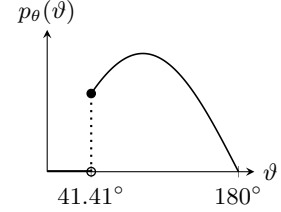


FIG. 10. The left-truncated sine model of the ensemble bond angle distribution for bulk liquid argon.

we arrive at an expression for the unnormalized XDF of an atom in bulk liquid argon at 85 K and 1 atm:

$$\begin{aligned} \hat{Z}_\varepsilon \hat{p}_\varepsilon(\varepsilon) &= \mathbf{1}\{\varepsilon = 0\} \sum_{\kappa=0}^2 p_k(\kappa) \\ &+ \frac{1}{\binom{54}{39}} \sum_{\kappa=3}^{17} \frac{\binom{17}{\kappa} \binom{37}{39-\kappa}}{\mathcal{S}(\kappa)} \exp \left\{ \left(\frac{\mathcal{H}(\varepsilon, \kappa) - \mathcal{M}(\kappa)}{\sqrt{2} \mathcal{S}(\kappa)} \right)^2 \right\}, \\ \varepsilon &\in \left\{ \log_2 \binom{a}{2} - b : a \in \mathbb{N}, 2 \leq a \leq 17, b \in \mathbb{H}_a \right\}; \end{aligned} \quad (54)$$

where the set \mathbb{H}_a is as defined in Eq. (20) and the auxiliary functions \mathcal{H} , \mathcal{M} , and \mathcal{S} are given respectively by

$$\begin{aligned} \mathcal{H}(\varepsilon, \kappa) &= \log_2 \binom{\kappa}{2} - \varepsilon, \\ \mathcal{M}(\kappa) &= \hat{\mu}_{H(\theta)|k}(\kappa) \\ &\approx \max \left\{ 0, 3.771 - \frac{14}{\kappa(\kappa-1) \ln 2} \right\}, \\ \mathcal{S}(\kappa) &= \hat{\sigma}_{H(\theta)|k}(\kappa) \\ &\approx \sqrt{\frac{0.123}{\kappa(\kappa-1)}}. \end{aligned}$$

This expression is plotted in Fig. 11.

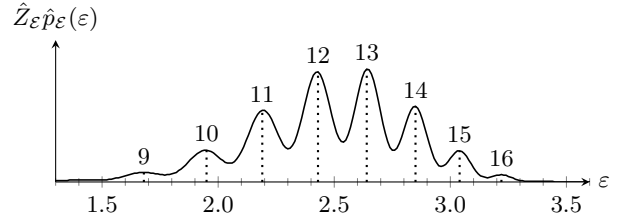


FIG. 11. Unnormalized XDF for liquid argon at 85 K and 1 atm, as predicted by $\hat{Z}_\varepsilon \hat{p}_\varepsilon$. Modal coordination numbers for the eight prominent peaks are indicated above the curve.

[1] S. Mehdi, Z. Smith, L. Herron, Z. Zou, and P. Tiwary, Enhanced sampling with machine learning, *Annu. Rev. Phys. Chem.* **75**, 347 (2024).

[2] L. Berthier and D. R. Reichman, Modern computational studies of the glass transition, *Nat. Rev. Phys.* **5**, 102 (2023).

[3] L. Bonati, G. Piccini, and M. Parrinello, Deep learning the slow modes for rare events sampling, *Proc. Natl. Acad. Sci. U.S.A.* **118**, e2113533118 (2021).

[4] M. I. Aroyo, U. Müller, and H. Wondratschek, Historical introduction, in *International Tables for Crystallography Volume A1: Symmetry relations between space groups*, edited by H. Wondratschek and U. Müller (Springer Netherlands, Dordrecht, 2004) pp. 2–5.

[5] C. Giacovazzo, C. Giacovazzo, H. L. Monaco, G. Artioli, D. Viterbo, M. Milanesio, G. Gilli, P. Gilli, G. Zanotti, G. Ferraris, and M. Catti, *Fundamentals of Crystallography* (Oxford University Press, 2011).

[6] C. J. Bradley and A. P. Cracknell, *The Mathematical Theory of Symmetry in Solids: Representation Theory for Point Groups and Space Groups* (Oxford University Press, 2010).

[7] C. Kittel, *Introduction to Solid State Physics*, 9th ed. (John Wiley & Sons, New York, NY, 2018).

[8] H. E. Fischer, A. C. Barnes, and P. S. Salmon, Neutron and x-ray diffraction studies of liquids and glasses, *Rep. Prog. Phys.* **69**, 233 (2005).

[9] S. Torquato, Hyperuniform states of matter, *Phys. Rep.* **745**, 1 (2018).

[10] J. D. Bernal, A geometrical approach to the structure of liquids, *Nature* **183**, 141 (1959).

[11] H. W. Sheng, W. K. Luo, F. M. Alamgir, J. M. Bai, and E. Ma, Atomic packing and short-to-medium-range order in metallic glasses, *Nature* **439**, 419 (2006).

[12] H. Tanaka, H. Tong, R. Shi, and J. Russo, Revealing key structural features hidden in liquids and glasses, *Nat. Rev. Phys.* **1**, 333 (2019).

[13] A. Stukowski, Structure identification methods for atomistic simulations of crystalline materials, *Model. Simul. Mater. Sci. Eng.* **20**, 045021 (2012).

[14] A. P. Bartók, R. Kondor, and G. Csányi, On representing chemical environments, *Phys. Rev. B* **87**, 184115 (2013).

[15] C. P. Royall and S. R. Williams, The role of local structure in dynamical arrest, *Phys. Rep.* **560**, 1 (2015).

[16] J.-P. Hansen and I. McDonald, *Theory of Simple Liquids: With Applications to Soft Matter*, 4th ed. (Academic Press, Amsterdam, 2013).

[17] R. Pathria and P. D. Beale, *Statistical Mechanics*, 3rd ed. (Academic Press, Oxford, UK, 2011).

[18] D. Coslovich, Static triplet correlations in glass-forming liquids: A molecular dynamics study, *J. Chem. Phys.* **138**, 12A539 (2013).

[19] T. A. Sharp, S. L. Thomas, E. D. Cubuk, S. S. Schoenholz, D. J. Srolovitz, and A. J. Liu, Machine learning determination of atomic dynamics at grain boundaries, *Proc. Natl. Acad. Sci. U.S.A.* **115**, 10943 (2018).

[20] Z. Zhang and W. Kob, Revealing the three-dimensional structure of liquids using four-point correlation functions, *Proc. Natl. Acad. Sci. U.S.A.* **117**, 14032 (2020).

[21] Y.-C. Hu and H. Tanaka, Revealing the role of liquid preordering in crystallisation of supercooled liquids, *Nat. Commun.* **13**, 4519 (2022).

[22] H. Tanaka, Structural origin of dynamic heterogeneity in supercooled liquids, *J. Phys. Chem. B* **129**, 789 (2025).

[23] Y. Jiao, F. H. Stillinger, and S. Torquato, Geometrical ambiguity of pair statistics. i. point configurations, *Phys. Rev. E* **81**, 011105 (2010).

[24] F. H. Stillinger and S. Torquato, Structural degeneracy in pair distance distributions, *J. Chem. Phys.* **150**, 204125 (2019).

[25] P. M. Maffettone, W. J. K. Fletcher, T. C. Nicholas, V. L. Deringer, J. R. Allison, L. J. Smith, and A. L. Goodwin, When can we trust structural models derived from pair distribution function measurements?, *Faraday Discuss.* **255**, 311 (2025).

[26] T. Nagler and C. Czado, Evading the curse of dimensionality in nonparametric density estimation with simplified vine copulas, *J. Multivar. Anal.* **151**, 69 (2016).

[27] J. D. Bernal, The bakerian lecture, 1962. the structure of liquids, *Proc. R. Soc. Lond. A Math. Phys. Sci.* **280**, 299 (1964).

[28] A. J. Baddeley and J. Møller, Nearest-neighbour markov point processes and random sets, *Int. Stat. Rev.* **57**, 89 (1989).

[29] P. J. Steinhardt, D. R. Nelson, and M. Ronchetti, Bond-orientational order in liquids and glasses, *Phys. Rev. B* **28**, 784 (1983).

[30] S. Torquato, B. Lu, and J. Rubinstein, Nearest-neighbor distribution functions in many-body systems, *Phys. Rev. A* **41**, 2059 (1990).

[31] E. Boattini, S. Marín-Aguilar, S. Mitra, G. Foffi, F. Smalleenburg, and L. Filion, Autonomously revealing hidden local structures in supercooled liquids, *Nat. Commun.* **11**, 5479 (2020).

[32] M. E. Fisher and D. Ruelle, The stability of many-particle systems, *J. Math. Phys.* **7**, 260 (1966).

[33] H. Tanaka, Bond orientational order in liquids: Towards a unified description of water-like anomalies, liquid-liquid transition, glass transition, and crystallization, *Eur. Phys. J. E* **35**, 113 (2012).

[34] S. N. Chiu, D. Stoyan, W. S. Kendall, and J. Mecke, *Stochastic Geometry and Its Applications*, 3rd ed., Wiley Series in Probability and Statistics (John Wiley & Sons, 2013).

[35] J. D. Martin, S. J. Goettler, N. Fossé, and L. Iton, Designing intermediate-range order in amorphous materials, *Nature* **419**, 381 (2002).

[36] T. Aste, M. Saadatfar, and T. J. Senden, The geometrical structure of disordered sphere packings, *Phys. Rev. E* **71**, 061302 (2005).

[37] W. L. Bragg and E. J. Williams, The effect of thermal agitation on atomic arrangement in alloys, *Proc. R. Soc. Lond. Ser. A-Contain. Pap. Math. Phys. Character* **145**, 699 (1934).

[38] J. M. Cowley, An approximate theory of order in alloys, *Phys. Rev.* **77**, 669 (1950).

[39] R. Kikuchi, A theory of cooperative phenomena, *Phys. Rev.* **81**, 988 (1951).

[40] J. Sanchez, F. Ducastelle, and D. Gratias, Generalized cluster description of multicomponent systems, *Phys. A: Stat. Mech. Appl.* **128**, 334 (1984).

[41] L. D. Landau and E. M. Lifshitz, *Statistical Physics, Part 1*, Course of Theoretical Physics, Vol. 5 (Pergamon Press, Oxford, 1980).

[42] J. P. Sethna, *Statistical Mechanics: Entropy, Order Parameters, and Complexity*, 2nd ed., Oxford Master Series in Physics (Oxford University Press, 2021).

[43] A. Baddeley, E. Rubak, and R. Turner, *Spatial Point Patterns: Methodology and Applications with R* (Chapman and Hall/CRC Press, London, 2015).

[44] M. N. M. van Lieshout, *Markov Point Processes and Their Applications* (Imperial College Press, London, 2000).

[45] E. M. Lifshitz and L. P. Pitaevskii, *Statistical Physics, Part 2: Theory of the Condensed State* (Pergamon Press, Oxford, 1980).

[46] R. E. Nettleton and M. S. Green, Expression in terms of molecular distribution functions for the entropy density in an infinite system, *J. Chem. Phys.* **29**, 1365 (1958).

[47] A. Baranyai and D. J. Evans, Direct entropy calculation from computer simulation of liquids, *Phys. Rev. A* **40**, 3817 (1989).

[48] L. Angelani and G. Foffi, Configurational entropy of hard spheres, *J. Phys.: Condens. Matter* **19**, 256207 (2007).

[49] A. Banerjee, S. Sengupta, S. Sastry, and S. M. Bhattacharyya, The role of structure and entropy in determining differences in dynamics for glass formers with different interaction potentials, *Phys. Rev. Lett.* **113**, 225701 (2014).

[50] S. Martiniani, K. J. Schrenk, J. D. Stevenson, D. J. Wales, and D. Frenkel, Turning intractable counting into sampling: Computing the configurational entropy of three-dimensional jammed packings, *Phys. Rev. E* **93**, 012906 (2016).

[51] Y. Zhou and S. T. Milner, Structural entropy of glassy systems from graph isomorphism, *Soft Matter* **12**, 7281 (2016).

[52] X. Yang, R. Liu, M. Yang, W. Wang, and K. Chen, Structures of local rearrangements in soft colloidal glasses, *Phys. Rev. Lett.* **116**, 238003 (2016).

[53] P. M. Piaggi and M. Parrinello, Entropy based fingerprint for local crystalline order, *J. Chem. Phys.* **147**, 114112 (2017).

[54] J. E. Hallett, F. Turci, and C. P. Royall, Local structure in deeply supercooled liquids exhibits growing length-scales and dynamical correlations, *Nat. Commun.* **9**, 3272 (2018).

[55] One choice can be obtained via singular value decomposition and the Gram matrix of the neighbor vector matrix.

[56] J. D. Bernal and J. L. Finney, Geometry of random packing of hard spheres, *Discuss. Faraday Soc.* **43**, 62 (1967).

[57] S. Torquato, T. M. Truskett, and P. G. Debenedetti, Is random close packing of spheres well defined?, *Phys. Rev. Lett.* **84**, 2064 (2000).

[58] S. Torquato and F. H. Stillinger, Jammed hard-particle packings: From kepler to bernal and beyond, *Rev. Mod. Phys.* **82**, 2633 (2010).

[59] A. Zaccone and E. Scossa-Romano, Approximate analytical description of the nonaffine response of amorphous solids, *Phys. Rev. B* **83**, 184205 (2011).

[60] S. S. Schoenholz, E. D. Cubuk, D. M. Sussman, E. Kaxiras, and A. J. Liu, A structural approach to relaxation in glassy liquids, *Nat. Phys.* **12**, 469 (2016).

[61] M. Laurati, P. Maßhoff, K. Mutch, S. Egelhaaf, and A. Zaccone, Long-lived neighbors determine the rheological response of glasses, *Phys. Rev. Lett.* **118**, 018002 (2017).

[62] C. Xia, J. Li, B. Kou, Y. Cao, Z. Li, X. Xiao, Y. Fu, T. Xiao, L. Hong, J. Zhang, W. Kob, and Y. Wang, Origin of non-cubic scaling law in disordered granular packing, *Phys. Rev. Lett.* **118**, 238002 (2017).

[63] H. Mizuno, K. Saitoh, and L. E. Silbert, Structural and mechanical characteristics of sphere packings near the jamming transition: From fully amorphous to quasi-ordered structures, *Phys. Rev. Mater.* **4**, 115602 (2020).

[64] V. Bapst, T. Keck, A. Grabska-Barwińska, C. Donner, E. D. Cubuk, S. S. Schoenholz, A. Obika, A. W. R. Nelson, T. Back, D. Hassabis, and P. Kohli, Unveiling the predictive power of static structure in glassy systems, *Nat. Phys.* **16**, 448 (2020).

[65] A. Zaccone, Explicit analytical solution for random close packing in $d = 2$ and $d = 3$, *Phys. Rev. Lett.* **128**, 028002 (2022).

[66] C. Anzivino, M. Casiulis, T. Zhang, A. S. Moussa, S. Martiniani, and A. Zaccone, Estimating random close packing in polydisperse and bidisperse hard spheres via an equilibrium model of crowding, *J. Chem. Phys.* **158**, 044901 (2023).

[67] D. Coslovich, Locally preferred structures and many-body static correlations in viscous liquids, *Phys. Rev. E* **83**, 051505 (2011).

[68] E. D. Cubuk, S. S. Schoenholz, J. M. Rieser, B. D. Malone, J. Rottler, D. J. Durian, E. Kaxiras, and A. J. Liu, Identifying structural flow defects in disordered solids using machine-learning methods, *Phys. Rev. Lett.* **114**, 108001 (2015).

[69] J. Russo and H. Tanaka, Crystal nucleation as the ordering of multiple order parameters, *J. Chem. Phys.* **145**, 211801 (2016).

[70] H. Tong and H. Tanaka, Revealing hidden structural order controlling both fast and slow glassy dynamics in supercooled liquids, *Phys. Rev. X* **8**, 011041 (2018).

[71] M. Harrington, A. J. Liu, and D. J. Durian, Machine learning characterization of structural defects in amorphous packings of dimers and ellipses, *Phys. Rev. E* **99**, 022903 (2019).

[72] E. Boattini, F. Smallenburg, and L. Filion, Averaging local structure to predict the dynamic propensity in supercooled liquids, *Phys. Rev. Lett.* **127**, 088007 (2021).

[73] S. N. Pozdnyakov and M. Ceriotti, Incompleteness of graph neural networks for points clouds in three dimensions, *Mach. Learn. Sci. Technol.* **3**, 045020 (2022).

[74] A. Dewaele, A. D. Rosa, N. Guignot, D. Andrault, J. E. F. S. Rodrigues, and G. Garbarino, Stability and equation of state of face-centered cubic and hexagonal close packed phases of argon under pressure, *Sci. Rep.* **11**, 15192 (2021).

[75] D. Chandler, *Introduction to Modern Statistical Mechanics* (Oxford University Press, New York, 1987) p. 274.

[76] M. E. Tuckerman, *Statistical Mechanics: Theory and Molecular Simulation*, 1st ed., Oxford Graduate Texts (Oxford University Press, Oxford, 2010).

[77] R. M. Gray, *Entropy and Information Theory*, 2nd ed. (Springer, New York, NY, 2011).

[78] C. E. Shannon, A mathematical theory of communication, *Bell Syst. Tech. J.* **27**, 379 (1948).

[79] T. M. Cover and J. A. Thomas, *Elements of Information Theory*, 2nd ed. (Wiley-Interscience, Hoboken, NJ, 2006).

[80] M. Boutin and G. Kemper, On reconstructing n-point configurations from the distribution of distances or areas, *Adv. Appl. Math.* **32**, 709 (2004).

[81] R. V. L. Hartley, Transmission of information, *Bell Syst. Tech. J.* **7**, 535 (1928).

[82] A. Y. Khinchin, *Mathematical Foundations of Information Theory*, Dover Books on Mathematics (Dover Publications, New York, 1957).

[83] J. Çamkıran, F. Parsch, and G. D. Hibbard, A local order parameter for systems of interacting particles, *J. Chem. Phys.* **156**, 091101 (2022).

[84] J. Çamkıran, F. Parsch, and G. D. Hibbard, On the topology of the space of coordination geometries, *Eur. Phys. J. B* **96**, 72 (2023).

[85] J. C. Stimać, C. Serrao, and J. K. Mason, Dependence of simulated radiation damage on crystal structure and atomic misfit in metals, *J. Nucl. Mater.* **585**, 154633 (2023).

[86] G. D. Hibbard and J. Çamkıran, Towards an information-based theory of structure, *Mater. Horiz.* **11**, 5464 (2024).

[87] R. B. King, Chemical applications of topology and group theory. iv. polyhedra for coordination numbers 10–16, *J. Am. Chem. Soc.* **92**, 7710 (1970).

[88] H. S. M. Coxeter, *Regular Polytopes*, 3rd ed. (Dover Publications, New York, 1973).

[89] F. C. Frank, Supercooling of liquids, *Proc. R. Soc. Lond. A* **215**, 43 (1952).

[90] H. Cohn and A. Kumar, Universally optimal distribution of points on spheres, *J. Amer. Math. Soc.* **20**, 99 (2007).

[91] A. Malins, S. R. Williams, J. Eggers, and C. P. Royall, Identification of structure in condensed matter with the topological cluster classification, *J. Chem. Phys.* **139**, 234506 (2013).

[92] T. C. Hales and S. McLaughlin, The dodecahedral conjecture, *J. Amer. Math. Soc.* **23**, 299 (2010), arXiv:math/9811079 [math.MG].

[93] F. M. Schaller, R. F. B. Weigel, and S. C. Kapfer, Densest local structures of uniaxial ellipsoids, *Phys. Rev. X* **6**, 041032 (2016).

[94] N. J. A. Sloane, R. H. Hardin, T. D. S. Duff, and J. H. Conway, Minimal-energy clusters of hard spheres, *Discrete Comput. Geom.* **14**, 237 (1995).

[95] V. N. Manoharan, M. T. Elsesser, and D. J. Pine, Dense packing and symmetry in small clusters of microspheres, *Science* **301**, 483 (2003).

[96] J. L. Finney, Local pseudosymmetry in simple liquids, *Comput. Math. Appl.* **17**, 341 (1989).

[97] M. Leocmach and H. Tanaka, Roles of icosahedral and crystal-like order in the hard spheres glass transition, *Nat. Commun.* **3**, 974 (2012).

[98] H. Tanaka, Importance of many-body orientational correlations in the physical description of liquids, *Faraday Discuss.* **167**, 9 (2013).

[99] Y. C. Hu, F. Li, M. Li, H. Y. Bai, and W.-H. Wang, Five-fold symmetry as indicator of dynamic arrest in metallic glass-forming liquids, *Nat. Commun.* **6**, 8310 (2015).

[100] M. Pinsky and D. Avnir, Continuous symmetry measures. 5. the classical polyhedra, *Inorg. Chem.* **37**, 5575 (1998).

[101] A. Gavezzotti, *Molecular Aggregation: Structure Analysis and Molecular Simulation of Crystals and Liquids* (Oxford University Press, Oxford, 2007).

[102] D. R. Nelson and B. I. Halperin, Dislocation-mediated melting in two dimensions, *Phys. Rev. B* **19**, 2457 (1979).

[103] C. L. Kelchner, S. J. Plimpton, and J. C. Hamilton, Dislocation nucleation and defect structure during surface indentation, *Phys. Rev. B* **58**, 11085 (1998).

[104] H. Tsuzuki, P. S. Branicio, and J. P. Rino, Structural characterization of deformed crystals by analysis of common atomic neighborhood, *Comput. Phys. Commun.* **177**, 518 (2007).

[105] J. Cumby and J. P. Attfield, Ellipsoidal analysis of coordination polyhedra, *Nat. Commun.* **8**, 14235 (2017).

[106] D. Han, D. Wei, J. Yang, H.-L. Li, M.-Q. Jiang, Y.-J. Wang, L.-H. Dai, and A. Zacccone, Atomistic structural mechanism for the glass transition: Entropic contribution, *Phys. Rev. B* **101**, 014113 (2020).

[107] A. C. Y. Liu, H. Pham, A. Bera, T. C. Petersen, T. W. Sirk, S. T. Mudie, R. F. Tabor, J. Núñez-Iglesias, A. Zacccone, and M. Baggio, Measurable geometric indicators of local plasticity in glasses, arXiv preprint 10.48550/arXiv.2410.09391 (2024), submitted Oct 12, 2024.

[108] J. A. Gallian, *Contemporary Abstract Algebra*, 10th ed. (CRC Press, Boca Raton, FL, 2021).

[109] K. Schütte and B. L. van der Waerden, Das problem der dreizehn kugeln, *Math. Ann.* **125**, 325 (1952).

[110] O. R. Musin, The kissing problem in three dimensions, *Discrete Comput. Geom.* **35**, 375 (2006).

[111] H. T. Croft, 9-point and 7-point configurations in 3-space, *Proc. Lond. Math. Soc.* **3**, **12**, 400 (1962).

[112] G. A. Miller, Note on the bias of information estimates, *Information Theory in Psychology: Problems and Methods*, 95 (1955).

[113] L. Paninski, Estimation of entropy and mutual information, *Neural Comput.* **15**, 1191 (2003).

[114] A. W. v. d. Vaart, *Asymptotic Statistics*, Cambridge Series in Statistical and Probabilistic Mathematics (Cambridge University Press, 1998).

[115] M. D. Rintoul and S. Torquato, Computer simulations of dense hard-sphere systems, *J. Chem. Phys.* **105**, 9258 (1996).

[116] C. P. Royall, A. A. Louis, and H. Tanaka, Measuring colloidal interactions with confocal microscopy, *J. Chem. Phys.* **127**, 044507 (2007).

[117] S. Pieprzyk, M. N. Bannerman, A. C. Braňka, M. Chudak, and D. M. Heyes, Thermodynamic and dynamical properties of the hard sphere system revisited by molecular dynamics simulation, *Phys. Chem. Chem. Phys.* **21**, 6886 (2019).

[118] Neglecting zero-point motion.

[119] T. C. Hales, A proof of the kepler conjecture, *Ann. Math.* **162**, 1065 (2005).

[120] E. Kaxiras and J. D. Joannopoulos, *Quantum Theory of Materials* (Cambridge University Press, Cambridge, 2019).

[121] F. C. Frank and J. S. Kasper, Complex alloy structures regarded as sphere packings. i. definitions and basic principles, *Acta. Crystallogr.* **11**, 184 (1958).

[122] G. J. Ackland and A. P. Jones, Applications of local crystal structure measures in experiment and simulation, *Phys. Rev. B* **73**, 054104 (2006).

[123] A. Thompson, L. Swiler, C. Trott, S. Foiles, and G. Tucker, Spectral neighbor analysis method for automated generation of quantum-accurate interatomic potentials, *J. Comput. Phys.* **285**, 316 (2015).

[124] H. Hwang, D. A. Weitz, and F. Spaepen, Direct observation of crystallization and melting with colloids, *Proc. Natl. Acad. Sci. U.S.A.* **116**, 1180 (2019).

[125] F. Turci, G. Tarjus, and C. P. Royall, From glass formation to icosahedral ordering by curving three-dimensional space, *Phys. Rev. Lett.* **118**, 215501 (2017).

[126] D. R. Nelson, *Defects and Geometry in Condensed Matter Physics* (Cambridge University Press, Cambridge & New York, 2002) pp. xiii + 377.

[127] H. B. Callen, *Thermodynamics and an Introduction to Thermostatistics*, 2nd ed. (John Wiley & Sons, New York, NY, 1985).

[128] T. S. Ingebrigtsen, T. B. Schrøder, and J. C. Dyre, What is a simple liquid?, *Phys. Rev. X* **2**, 011011 (2012).

[129] E. Greene and J. A. Wellner, Exponential bounds for the hypergeometric distribution, *Bernoulli* **23**, 1911 (2017).

[130] J. D. Bernal and J. Mason, Packing of spheres: Coordination of randomly packed spheres, *Nature* **188**, 910 (1960).

[131] G. D. Scott and D. M. Kilgour, The density of random close packing of spheres, *Journal of Physics D: Applied Physics* **2**, 863 (1969).

[132] J. L. Yarnell, M. J. Katz, R. G. Wenzel, and S. H. Koenig, Structure factor and radial distribution function for liquid argon at 85 °k, *Phys. Rev. A* **7**, 2130 (1973).

[133] A. V. Anikeenko, G. G. Malenkov, and Y. I. Naberukhin, Visualization of the collective vortex-like motions in liquid argon and water: Molecular dynamics simulation, *J. Chem. Phys.* **148**, 094508 (2018).

[134] A. L. Mackay, A dense non-crystallographic packing of equal spheres, *Acta Crystallogr.* **15**, 916 (1962).

[135] T. P. Martin, Shells of atoms, *Phys. Rep.* **273**, 199 (1996).

[136] N. Canestrari, D. Nelli, and R. Ferrando, General theory for packing icosahedral shells into multi-component aggregates, *Nat. Commun.* **16**, 1655 (2025).

[137] J. D. Weeks, D. Chandler, and H. C. Andersen, Role of Repulsive Forces in Determining the Equilibrium Structure of Simple Liquids, *J. Chem. Phys.* **54**, 5237 (1971).

[138] F. A. Lindemann, Über die berechnung molekulärer eigenfrequenzen, *Physikalische Zeitschrift* **11**, 609 (1910).

[139] P. Lunkenheimer, A. Loidl, B. Riechers, A. Zaccione, and K. Samwer, Thermal expansion and the glass transition, *Nat. Phys.* **19**, 694 (2023).

[140] F. Saija, S. Prestipino, and P. V. Giaquinta, Evaluation of phenomenological one-phase criteria for the melting and freezing of softly repulsive particles, *J. Chem. Phys.* **124**, 244504 (2006).

[141] M. Oettel, S. Görig, A. Härtel, H. Löwen, M. Radu, and T. Schilling, Free energies, vacancy concentrations, and density distribution anisotropies in hard-sphere crystals: A combined density functional and simulation study, *Phys. Rev. E* **82**, 051404 (2010).

[142] V. N. Novikov and A. P. Sokolov, Role of quantum effects in the glass transition, *Phys. Rev. Lett.* **110**, 065701 (2013).